Universidad Nacional de Colombia - Sede Medellín

Master's Thesis

Improvement of the performance of a hydrocracking reactor using a computational fluid dynamics perspective.

Author:
Juan José Arias Belduque

Supervisor:
Alejandro Molina

Thesis presented as a partial requirement to obtain the degree of:
M.Sc. in Chemical Engineering

Research Group: Bioprocesos y Flujos reactivos
Facultad de Minas, Departamento de Procesos y Energía

Medellín, Colombia
2015

Universidad Nacional de Colombia - Sede Medellín

Tesis de Maestría

Mejoramiento del funcionamiento de un reactor de hidrocraqueo usando una perspectiva de dinámica de fluidos computacional

Autor:
Juan José Arias Belduque

Supervisor:
Alejandro Molina

Tesis presentada como requisito parcial para obtener el título de:
Magíster en Ingeniería Ingeniería Química

Grupo de investigación: Bioprocesos y Flujos reactivos
Facultad de Minas, Departamento de Procesos y Energía

Medellín, Colombia
2015

UNIVERSIDAD NACIONAL DE COLOMBIA - SEDE MEDELLÍN

Abstract

Facultad de Minas

Facultad de Minas, Departamento de Procesos y Energía

M.Sc. in Chemical Engineering

Improvement of the performance of a hydrocracking reactor using a computational fluid dynamics perspective.

by Juan José Arias Belduque

The distribution of the liquid phase at the top of the catalytic bed of a hydrocracking trickle bed reactor was obtained by CFD simulations and coupled to a 1-D hydrocracking reactor model, used to evaluate the performance of the reactor. The design of the distribution system, that operated at industrial conditions ($644K$ and $17MPa$), was based on a multiphase CFD study carried out with the commercial software ANSYS Fluent v.15. Three CFD simulations were needed to accurately describe the distribution at the top of the reactor: (1) the gas phase entering to the vapor lift distributor (VLD) unit, a device used to mix the gas and the liquid phases; (2) the VLD itself, and (3) the dispersion zone where a mixture of both phases falls to the top of the catalyst bed from the outlet of the VLD unit. The CFD simulations and the 1-D hydrocracking reactor model were validated using literature data. A parameter variation process was done at the VLD unit and the dispersion zone, to improve the distribution of the liquid phase at the top of the catalytic bed and the performance of the hydrocracking reactor. For the VLD unit the parameter varied was the ratio between the separation plate height and the total VLD height. A comparison of three different cases showed that a value of 0.83 is the best configuration. The evaluation of two different depth distances for the dispersion zone indicates that $40cm$ offered the best liquid distribution at the top of the bed. With the configurations selected an analysis of different profiles at the top of the catalyst bed, showed the advantage of a careful description of the distribution in the top tray when predicting reactor conversion. An arrangement of VLD units allowed for a conversion of 0.1284 for conditions selected, which is comparable with obtained for the completely mixed case. These results indicate the importance of a proper description of the distribution system in this type of reactors.

UNIVERSIDAD NACIONAL DE COLOMBIA - SEDE MEDELLÍN

Resumen

Facultad de Minas

Facultad de Minas, Departamento de Procesos y Energía

M.Sc. in Chemical Engineering

Mejoramiento del funcionamiento de un reactor de hidrocraqueo usando una perspectiva de dinámica de fluidos computacional

por Juan José Arias Belduque

La distribución de la fase líquida en la parte superior del lecho catalítico de un reactor de hidrocraqueo se obtuvo mediante simulaciones CFD y acoplado con un modelo 1-D para un reactor de hidrocraqueo, se evaluó el desempeño del reactor. El sistema de distribución, operando a condiciones industriales (644 K and 17 MPa), se basó en un estudio CFD multifásico y se llevó a cabo usando el software ANSYS Fluent v.15. Tres simulaciones CFD fueron necesarias para describir correctamente la distribución en la parte superior del reactor: (1) el gas entrando a la unidad de distribución asistida por gas (VLD singlas en inglés), un dispositivo usado para mezclar las fases líquida y gas; (2) la unidad VLD en si misma, y (3) la zona de dispersion donde una mezcla de las dos fases cae a la parte superior del lecho catalíco desde la salida de la unidad VLD. Los resultados de la simulación CFD y los del modelo 1-D de un reactor de hidrocraqueo fueron validados usando datos de la literatura. Un proceso de variación de parámetros se realizó para la unidad VLD y para la zona de dispersión para mejorar la distribución de la fase líquida en la parte superior del lecho catalítico y el desempeño del reactor de hidrocraqueo. Para la unidad VLD el paramétro variado fue la altura de la placa separadora con respecto a la altura total de la unidad VLD. Una comparación entre tres casos diferentes mostró que un valor 0.83 es la mejor configuración. La evaluación de dos profundidades diferentes para la zona de dispersión indicó que $40cm$ ofrece la mejor distribución en la parte superior del lecho. Con las configuraciones seleccionadas un análisis de diferentes perfiles en la parte superior del lecho catalítico, mostró las ventajas de la cuidadosa descripción de la distribución en la parte superior cuando se predice la conversión del reactor. Un arreglo de unidades VLD permite una conversión de 0.1284 para las condiciones seleccionadas, que es comparable con la obtenida para el caso completamente mezclado. Estos resultados indican la importancia de la descripción apropiada de los sistemas de distribución en este tipo de reactores.

Acknowledgements

I would like to thank my parents, my sibling, my friends and my girlfriend for the constant support along this process.I would like to thank my partners at the research group for their advices, comments and specially for their friendship. I would like specially thank to professor Alejandro Molina because without his guidance and advices this thesis don't be possible.

And last but not least I would like to thank to Ecopetrol and Colciencias to fund this research work by the project: Development of simulations tools to heavy oil refinement - an approximation by computational fluid dynamics (CFD).

Contents

Abstract i

Resumen i

Acknowledgements iii

List of Figures vi

List of Tables ix

Abbreviations x

Physical Constants xi

Symbols xii

1 Introduction 1
- 1.1 Justification . . . 1
- 1.2 Objectives . . . 2
  - 1.2.1 General objective . . . 2
  - 1.2.2 Specific objectives . . . 2
- 1.3 Theoretical framework . . . 2
  - 1.3.1 Hydroprocessing . . . 2
  - 1.3.2 Hydrocracking process . . . 3
    - 1.3.2.1 Reactor configuration . . . 3
    - 1.3.2.2 Catalyst functioning . . . 4
  - 1.3.3 Multiphase models . . . 4
    - 1.3.3.1 ANSYS Fluent Volume of fluid (VOF) model . . . 4
    - 1.3.3.2 ANSYS Fluent Eulerian multiphase model . . . 4
  - 1.3.4 Maldistribution factor . . . 5
- 1.4 State of the Art . . . 5
- 1.5 Thesis outline . . . 7

2 Methodology 9
- 2.1 Bottleneck identification process . . . 9

2.2 CFD simulation process 10
2.2.1 Validation process 10
2.3 Evaluation of design configurations process 11

3 Bottleneck identification 12
3.1 Bottleneck to a VGO-hydrocracking process 12
3.2 Bottleneck implications to the CFD simulation process 13

4 CFD simulation of gas inlet to a single VLD unit 15
4.1 CFD modeling 15
4.1.1 Geometry, fluid properties, operating and boundary conditions . . 17
4.2 CFD simulation results 18

5 CFD simulation of a vapor lift distributor unit 22
5.1 CFD modeling 22
5.1.1 Geometry, fluid properties, operating and boundary conditions . . 23
5.2 Validation process 25
5.3 CFD simulation results 27

6 CFD simulation of the dispersion zone 31
6.1 CFD modeling 31
6.1.1 Geometry, fluid properties, operating and boundary conditions . . 32
6.2 Validation process 33
6.3 CFD simulation results 35

7 Parameter variation processes to enhance the liquid distribution 41
7.1 Parameter variation process over the VLD unit 41
7.2 Parameter variation process over the dispersion zone 43

8 Assessment of performance of a 1-D VGO-hydrocracking reactor using a non-homogeneous inlet profile 46
8.1 Model development 47
8.1.1 Assumptions 47
8.1.2 Fluid properties 48
8.2 Validation process 51
8.3 CFD modeling 54
8.4 Results 55

9 Conclusions 62

Bibliography 64

List of Figures

4.1 VLD unit operating scheme. Flow lines of the gas phase inside the VLD unit. . . . 16
4.2 Mesh used in the CFD simulation of the gas inlet at the VLD unit. 16
4.3 Tracking of the average velocity the slot inlet to idenfity when the simulation is on PSS. . . . 18
4.4 Behavior of the velocity magnitude. The vertical axis is logarithmic, while the horizontal axis is the ratio between X distance measured from the slot and the width of the VLD unit. . . . 19
4.5 Velocity profile in the height direction. The dimensionless variable on the vertical axis is the ratio between the y distance and the height of the slot. 19
4.6 Velocity contours of the gas phase as goes inside the VLD unit. 21
4.7 Velocity magnitude profile of the gaseous phase at the inlet slot profile. . 21

5.1 Mesh used in the simulation of the VLD unit with refinement in front of the inlet slot. . . . 23
5.2 ASTM D1160 distillation curve for the VGO. . . . 24
5.3 CFD simulation of the gas phase to validate the pressure drop on the VLD unit. . . . 26
5.4 Comparison between the data measured by Nolin and the CFD simulation results when the inlet slot area is equal to $3cm^2$ . . . 26
5.5 Comparison between the data measured by Nolin and the CFD simulation results when the inlet slot area is varied. . . . 27
5.6 Iso-surface of liquid phase volume fraction at different times. 28
5.7 VLD unit liquid phase volume fraction profile along the inlet leg. 29
5.8 VLD unit liquid phase volume fraction profile along the outlet leg. 30

6.1 500k non-homogeneous hexahedral cells mesh of the dispersion zone. . . . 32
6.2 Liquid volume fraction profile at the velocity inlets in the dispersion zone CFD simulation. . . . 34
6.3 Velocity profile at the velocity inlets in the dispersion zone CFD simulation. 34
6.4 Comparison between experimental data measured by Du et al., 2014 and calculated data. . . . 36
6.5 Liquid volume fraction profile above the top of the catalyst bed. 37
6.6 Stream lines from the velocity inlet boundary condition colored by the liquid volume fraction of the liquid phase. . . . 37
6.7 Liquid volume fraction distribution over the top of the catalyst bed. . . . 38
6.8 Liquid volume fraction distribution 2.5 cm below the top of the catalyst bed. . . . 38
6.9 Liquid volume fraction distribution 5 cm below the top of the catalyst bed. 39

6.10 Contour of the superficial velocity magnitude of the liquid phase in $m.s^{-1}$, over the top of the catalyst bed. . . . 39
6.11 Contour of the superficial velocity magnitude of the liquid phase in $m.s^{-1}$, $2.5cm$ below the top of the catalyst bed. . . . 40
6.12 Contour of the superficial velocity magnitude of the liquid phase in $m.s^{-1}$, $5cm$ below the top of the catalyst bed. . . . 40

7.1 Geometry changes done by change the ratio of separator wall height (SH) to total VLD unit height (H) . . . 42
7.2 Comparison of the liquid distribution at the outlet of the VLD unit through nine partitions when the ratio of separator wall (SH/H) changes over time. . . . 43
7.3 Liquid volume fraction distribution over the top of the catalyst bed, simulation with a depth of $20cm$. . . . 43
7.4 Liquid volume fraction distribution over the top of the catalyst bed, simulation with a depth of $40cm$. . . . 44
7.5 Liquid flow distribution in 9 planes at the top of the catalyst bed to the simulation domain with 20cm of depth. . . . 44
7.6 Liquid flow distribution in 9 planes at the top of the catalyst bed to the simulation domain with 40cm of depth. . . . 45
7.7 Velocity profile of the liquid phase above the top of the catalyst bed. . . . 45

8.1 Reaction mechanism used on the 1-D simulation of VGO-hydrocracking reactor. . . . 46
8.2 Dispersion plot of the API grades found in literature for different peusocomponents of the hydrocracking process. . . . 49
8.3 Dispersion plot of the ASTM D86 found in literature for different peusocomponents similar to Distillates of the hydrocracking process. Data number: 1-[35], 2-[36], 3-[37], 4-[3], 5-[38], 6-[38]. . . . 49
8.4 Dispersion plot of the ASTM D86 found in literature for different peusocomponents similar to Naphtha of the hydrocracking process. Data number: 1-[35], 2-[36], 3-[37], 4-[3], 5-[38], 6-[38]. . . . 50
8.5 TBP curves used to obtain the properties of the lumps in the hydrocracking reaction mechanism. Distillate and naphtha are ASTM D86 curves and Feed curve is an ASTM D1160 . . . 50
8.6 Parity plot of the mass balance, comparison between the calculated data against the experimental data measured by Mohanty. . . . 53
8.7 Parity plot of the energy balance, comparison between the calculated data against the experimental data measured by Mohanty. . . . 53
8.8 Liquid volume fraction profile obtained after an averaging process to different times. . . . 54
8.9 Velocity profile obtained after an averaging process to different times. . . . 55
8.10 Conversion in function of the residence time to cells randomly selected in the cases evaluated. . . . 57
8.11 Conversion in function of the temperature to cells randomly selected in the cases evaluated. . . . 57
8.12 Yield of the distillates in function of the temperature to cells randomly selected in the cases evaluated. . . . 58

8.13 Yield of the distillates in function of conversion of the feedstock to cells randomly selected in the cases evaluated. 58
8.14 Temperature at the outlet of the 1-D VGO-hydrocracking reactor model as function of the residence time. 59
8.15 Distribution plot of temperatures at the outlet of the 1-D VGO-hydrocracking model. 60
8.16 Evaluated cases compared against a profile with a high maldistribution in a plot of conversion as function of the mass flux of the feedstock at the inlet. 60
8.17 Evaluated cases compared against a profile with a high maldistribution in a plot of conversion as function of the residence time. 61

List of Tables

1.1 Range of operation conditions proposed by Gruia [3] to hydrocracking and hydrotreating processes 3

4.1 Gaseous phase properties on gas inlet to a single VLD unit simulation. . . 17

5.1 Properties of the liquid and gas phase in the VLD unit CFD simulation. . 24

6.1 Properties used on the porous zone in the simulation domain. 33

7.1 Change of the Maldistribution factor at the outlet of the VLD unit when the ratio of separator wall (SH/H) changes over time. 42

8.1 Correlations used by Aspen HYSYS to characterize a pseudo-component. 51
8.2 Kinetic constants of the four lumps mechanism reaction to hydrocracking of VGO 51
8.3 Global values of conversion, and products yields to the evaluated cases. . 57

Abbreviations

CFD	**C**omputational **F**luid **D**ynamics
TBR	**T**ricle **B**ed **R**eactor
VLD	**V**apor **L**ift **D**istributor
HDC	**H**y**D**ro**C**racking
PSS	**P**seudo-**S**tationary **S**tate
VGO	**V**acuum **G**as **O**il

Physical Constants

Gravity	g	$=$	$9.81\ m\ s^{-2}$
Gas constant	R	$=$	$8.314\ m^3\ Pa\ K^{-1}\ mol^{-1}$

Symbols

C	Heat capacity	$kJ\ kg^{-1}.^oC^{-1}$
E	Activation energy	$kJ\ mol^{-1}$
F	Mass flow	$kg\ h^{-1}$
H	Enthalpy	$kJ\ kg^{-1}$
P	Pressure	Pa
R	Rate of consumption(production)	$kg\ m^{-}3.h^{-}1$
T	Temperature	K
V	Volume	m^3
ρ	Mass density	$kg\ m^{-3}$
μ	Viscosity	$kg.\ m^{-1}.s^{-1}$
α	Volume fraction	
γ	Reaction rate	$kg\ m^{-}3.h^{-}1$
ζ	Stoichiometric coefficient	

A mis padres y hermanos.

Chapter 1

Introduction

1.1 Justification

The UPME (Mining and Energy Planning Unit by its spanish acronym) is a special administrative colombian unit that is responsible to develop plans to mining and energy sector. *Scenarios for Oil Supply and Demand in Colombia* is an official document presented by the UPME, the base-case scenario of this document shows that for the next twenty years is estimated that 1.205 million of heavy oil barrels (MBls) will be added to Colombia's oil reserves [1]. It is expected that a part of this new heavy oil reserves will be processed at local refineries, this kind of oil is characterized by a high viscosity and high density, hence to be refined much severe operating conditions are needed [1], knowledge about refining processes involved on the conversion of these heavy oils to more valuable products will be fundamental to compete on the global markets.

This thesis is part of the objectives proposed for the research project *Development of simulations tools to heavy oil refinement - an approximation by computational fluid dynamics (CFD)* funded by Ecopetrol and Colciencias, with the aim of strengthen national research groups on knowledge about heavy crude oil refining processes. Particularly, the aim of this research is to generate knowledge and achieve an improvement over the performance of a hydrocracking (HDC) process by studying the phenomenological interactions using a computational fluid dynamic (CFD) perspective.

1.2 Objectives

1.2.1 General objective

To propose design alternatives to improve the operation of a VGO-hydrocracking reactor.

1.2.2 Specific objectives

- To identify bottlenecks in the standard operation of a VGO-hydrocracking process reactor.
- To develop a computational fluid dynamic simulation of a VGO-hydrocracking process reactor.
- To evaluate different design configurations to improve the operation of a VGO-hydrocracking process reactor.

1.3 Theoretical framework

In this section will described some concepts that will be important along the document.

1.3.1 Hydroprocessing

Hydroprocessing is an oil refining process applied to heavy oil fractions with high concentrations of impurities. In this kind of process molecular hydrogen is fed at inlet stream with with two different objectives:

- To remove impurities in the feedstock mainly heteroatoms like N, O, V, Ni, and any other type of metals present on the hydrocarbon molecules which are replaced with hydrogen atoms.
- To decrease the molecular weight of the molecules into the feedstock, this change in the molecular weight is related to a change in the chemical identity of the molecules.

These processes are called hydrotreating and hydrocracking, respectively [2]. Typical conditions to this kind of processes were proposed by Gruia [3] and are summarized at the Table 1.1.

TABLE 1.1: Range of operation conditions proposed by Gruia [3] to hydrocracking and hydrotreating processes

Condition	**Hydrocracking**	**Hydrotreating**
Temperature (^oC)	300- 425 (572-797 ^oF)	290 379 (554-714.2 ^oF)
Partial pressure of H_2 (kPa)	8618 17236 (1250-2500 psi)	1378 13789 (200-2000 psi)
LHSV (h^{-1})	0.2 a 8	

1.3.2 Hydrocracking process

1.3.2.1 Reactor configuration

The configuration of HDC reactors can vary from one to another, but there are some similarities between them; excepting some novel configurations HDC processes are usually hosted in trickle bed reactors (TBR) [4], in this kind of configuration the catalyst is a fixed bed (with a porosity of 0.38 approximately) and the liquid trickles over the surface of the catalyst particles in a down-flow mode while it is exposed to a hydrogen atmosphere [5, 6]. The HDC reactions are exothermic, this means that reactions release energy as heat when they take place, this heat release is used to enhance the reaction rates of HDC process by an adiabatic operation. To control the temperature inside the HDC reactor a fluid (in HDC process is commonly used hydrogen or feedstock as quench fluid) is injected in the middle of two fixed beds, the injected fluid has a lower temperature than mixture exiting from first catalyst bed, this process is know as quenching process; thereby a typical configuration of a HDC reactor should have more than one fixed bed.

Another important component of the HDC process is the liquid distribution system. In the system are included the *distribution tray section*, that is a set of devices used to mix the phases and the *dispersion zone*, that is a non-catalyst zone located between the distribution tray and the top of the first catalyst bed, more specifically the *dispersion zone* is used to guarantee a good dispersion of the liquid/gas mixture that gets out from the VLD unit.

In conclusion, a HDC process can be separated in two zones: (1) the **liquid distribution zone** that includes all the reactor systems that are used to mix the phases and spread the liquid over the top of first catalyst bed and (2) the **reaction zone** that is the volume right below distribution zone full of catalyst and where the reactions take place. The interaction between both zones is located at the top of the catalyst bed.

1.3.2.2 Catalyst functioning

The HDC reactions take place over the surface of a catalyst, for this kind of process is used a mixed catalyst, it is called mixed because it is possible to find over the catalyst surface active sites with metallic components or acid components. The metallic sites are only composed by noble metals like palladium and platinum or metals in the group VIB and VIIIB (their oxides or sulphides); the last ones have a better tolerance to the presence of sulfur atoms in the feedstock, nevertheless they have less catalytic activity than their counterpart (noble metals). The main function of metallic sites is to activate the hydrogen and to catalyze the hydrogenation and dehydrogenation reactions. On the other hand, the acid sites have a cracking function by breaking bonds in the hydrocarbon molecules, these sites are composed by amorphous oxides, zeolites or mixtures of them. The concentration of metallic sites and acid sites in the catalyst depends on process needs [2, 3].

1.3.3 Multiphase models

1.3.3.1 ANSYS Fluent Volume of fluid (VOF) model

The VOF model was formulated under the assumption that modeling fluids are immiscible, this assumption allows to model two or more fluids by solving a single set of momentum equations. For each additional phase added to the simulation a new variable is introduced: the volume fraction of the phase in the computational cell. Using those variables it is possible to track the interface between phases through space and time, because the sum of the volume fraction of the phases must be equal to one. Due to a single set of momentum equations is solved, the velocity field obtained is shared among the phases. The set of momentum equation has a dependency on the volume fractions of all phases which is represented by the density (ρ) and viscosity (μ), as can be seen at the equation below (with a χ property), a property can be calculated using the volume fractions of all phases α_q at each cell.

$$\chi = \sum \alpha_q \chi_q \tag{1.1}$$

1.3.3.2 ANSYS Fluent Eulerian multiphase model

The Eulerian multiphase ANSYS model assumes that each of the phases can be simulated using an Eulerian treatment, this assumptions allows to simulate multiple separate and yet interacting phases, those phases could be any combination of liquids, gases or solids;

the only limitation of the Eulerian multiphase model for the number of secondary phases are: the memory requirements and convergence behavior for complex multiphase flows. In particular to this model a single pressure is shared by all phases and the momentum and continuity equations are solved for each phase. The Eulerian multiphase model can describe a multiphase flow as a continua by adding the volume fraction of each phase, also the interaction among the phases for the exchange of momentum, heat, and mass can be introduced.

1.3.4 Maldistribution factor

The maldistribution factor (M_f) proposed by Marcandelli in 2000 is a coefficient used on TBR simulation to quantify the uniformity of the liquid distribution. M_f is obtained by dividing a surface in the simulation domain in N zones with equal area, measuring the liquid flow rate through each of zones with equal area(Q_{Li}) and calculating the average liquid flow rate(Q_{Lmean}) with the total liquid flow rate through the selected surface and total number equal areas (N) [7] with the equation below.

$$Q_{Lmean} = \frac{Q_{Ltotal}}{N} \tag{1.2}$$

The maldistribution coefficient (M_f) is defined as:

$$M_f = \sqrt{\frac{1}{N(N-1)} \sum \left(\frac{Q_{Li} - Q_{Lmean}}{Q_{Lmean}} \right)^2} \tag{1.3}$$

The M_f coefficient varies from 1 for a perfect distribution of liquid at the surface to 0 if the liquid only flows using a single zone of equal area of the surface. Thus, until lower the value of M_f the better of the liquid distribution at the surface selected.

1.4 State of the Art

As stated previously, the hydrocracking reactions are usually hosted on TBRs, this kind of reactors have been modeled since mid-70s when Satterfield [8] proposes the first simulation of a TBR using empirical correlations to approximate the flow regime, the pressure drop, liquid hold up, mass coefficients and other important parameters. It was at 1999 with Jiang et al. work that a CFD simulation of a TBR was built to observe the flow distribution of two phases in a 2-D model [9].

In 2003, Ranade proposes a methodology to model a TBRs using an Eulerian multiphase model coupled with models for wetting efficiency, interphase momentum exchange, porous distribution and capillary pressure [10], this methodology is used to nowadays. Along the years different works (as examples: [11–13]) were published using different models to those variables. One of the most widespread models to inter-phase momentum exchange is the model proposed by Attou et al., this model became popular on TBR CFD simulation because it was developed via force balances and it has good agreement with experimental data [14].

In 2007, Ranade sets the first approach to model a reactive multiphase flow in a TBR using a CFD simulation [15]. This same approach with some variations is still being used to simulate reactive flux on TBR, as example are Hashemabadi works, where hydrotreating of gasoil in a TBR is simulated isothermally and non-isothermally [16, 17].

Liquid spreading at the inlet and inside TBRs has been extensively studied experimentally as showed by Marcandelli [7], Moller [18], Nigam [19], Tsochatzidis [20] works. In particular the research work done by Marcandelli et al. lay the foundation to analyze the liquid maldistribution by proposing the Maldistribution factor, a coefficient that is calculated using the liquid flows in different sections of the reactor [7]. In 2005 Boyer et al. presented a research work in liquid spreading in TBR with an experimental component and a CFD simulation, this work marks the beginning of CFD simulation of liquid spreading and liquid distribution in TBRs [11].

After Boyer et al research work, CFD simulations with non-homogeneous inlet of liquid are developed; Atta et al. [21] developed a 3-D CFD simulation using the porous media concept with only two phases (rather than three-phase Eulerian model) to capture the liquid flow maldistribution experimentally measured by Marcandelli in 2000. Bazmi et al. (2012) studied the liquid flow maldistribution in a TBR using different configurations to liquid entrance [22], with the traditional three-phase Eulerian approach and compares the results against Atta et al. results. Solomenko (2015)[23] using a two Eulerian approach studied the liquid distribution in a TBR with a 2-D and 3-D CFD simulations besides it was developed a sensitivity analysis of the liquid spreading to different variables. In 2012, Kuzeljevic et al. developed a CFD simulation that can be consider the first research work with a reactive flow and liquid distribution components, because the liquid inlet was simulated using injection points instead of a homogeneous profile and the reaction of decomposition of hydrogen peroxide in cooper chromite catalyst was modeled [24].

All the previous research works generate important knowledge of TBR operation in their own way but all have in common that to spread the liquid it was used the distribution tray technology; as Maiti summarized in 2007 there are different kinds of gas-liquid

distributors for TBRs and the distribution tray technology is being replaced by new developments [25]. In 2015, Augier et al. in their review work done to the oil and gas industry [26] considers that the CFD simulation of gas-liquid distributors is a topic with an increasing trend because there are new requirements for the industry to take advantage of the reactive volume in the TBRs, which only can be done by the enhancing the liquid distribution at the top of the catalyst beds. The works done by Ramajo [27] and Martinez [28] simulated a perforated plate and chimney in a distribution tray, respectively, both works focused in accurately describe the behavior of the phases at the inlet of the TBRs.

There is no CFD simulations of VLD units in the open literature at the time of this thesis but the experimental works of Du et al. [29] and Nolin [30] could be the starting point to develop a CFD simulation of a VLD unit, both works have a lot of experimental measurements to gas flows. Besides Du et al. describes some important patterns in the VLD unit operation, as well as gives operation ranges to some important variables to the correctly operation of the VLD unit. It is important to note that both works have a lack of information about the geometry of the VLD unit, even though this issue can overcome using data reported in other works like the Bazer-Bachi experimental work done with gas-liquid distributors [31], this lack of information makes more difficult the CFD process simulation.

1.5 Thesis outline

This document is divided in 9 chapters, in the first chapter there is an introduction to VGO-hydrocracking process, important concepts for the thesis and a brief state of the art are presented. In the second chapter is presented the general methodology used in this thesis to complete the proposed objectives; each of simulation chapters explain extensively how each simulation was done, the conditions used, the assumptions made and the simulation results. In the third chapter an analysis of the literature suggests that liquid maldistribution is a relevant bottleneck to the TBR and VGO-hydrocracking operation is introduced, in this chapter is also explained the implications of the identified bottleneck to the CFD simulation process done in this thesis.

The next three chapters are focused on the systems that were studied: (1) the gas inlet to the VLD unit (Chapter 4), (2) the VLD unit itself (Chapter 5) and (3) the dispersion zone (Chapter 6). The seventh chapter summarized the geometrical changes done over the CFD simulations to enhance the liquid distribution at the top of the catalyst bed when is used a VLD unit to mix the phases.

The best configurations found in the Chapter 7 were used to build a simulation in the Chapter 8, the liquid distribution obtained in the simulation was analyzed using a 1-D mathematical model of a VGO-hydrocracking reactor besides some strategies used on the previous chapters (Chapter 8).

Finally, in the last chapter are the general conclusions obtained from this work.

Chapter 2

Methodology

In this chapter it will detailed the general methodology used to achieve the specific objectives proposed previously, this chapter is divided in three sections: Bottleneck identification process section, the CFD simulations process section and evaluation of design configurations process section.

In the bottleneck identification process section is explained the methodology used to identify a relevant bottleneck that could be simulated via CFD. In the CFD simulations section is detailed the simulation process done, the software used and the validation process, but the particularities of each simulation are extensively explained in each simulation chapter. Finally in the evaluation of design configurations process section there are explained the strategies used to evaluate the liquid distribution in the CFD simulations and there is an emphasis in the evaluation of the liquid distribution at the top of the catalyst bed.

2.1 Bottleneck identification process

The bottleneck detected to the VGO-hydrocracking operation was identified by a searching in open literature, a first search was done to find any problem on reactor operation regardless if was possible to be addressed using a CFD simulation. After, a second search was done but it was limited to find only operational issues that could involve a CFD simulation, this search suggested that an attractive bottleneck to be solve via CFD simulation it must be associated with TBRs operation. At the chapter 3 are presented the results of the second search, these are the results related only to TBR operation.

2.2 CFD simulation process

After being identified the bottleneck in the VGO-hydrocracking process the next step is to formulate the CFD simulation, the CFD simulations were built using ANSYS Fluent v.15, there are different kind of models available to be used on ANSYS Fluent v.15; the state of the art suggests that the best way to model the behavior of the phases at any stage of the VGO-hydrocracking process is by multiphase models accordingly to the requirements of the simulation a model of this kind was selected to the simulation process. The meshes needed were built using ICEM CFD v.15 a meshing program available on ANSYS v.15.

Process data like operating conditions, properties of the fluids, HDC kinetic constants, global conversion and products yields were obtained before starting the simulation process. Some of this information (operating conditions, global conversion and products yields) was took from the work done by Mohanty in 1991 for a two step-hydrocracking reactor [32]. The properties of the fluids were obtained using ASPEN HYSYS; the complex components like the feedstock and the products of the HDC process which are mixtures of thousands different organic molecules with different number of carbons and H/C ratio were characterized by using a pseudo-component, in ASPEN HYSYS to characterize a pseudo-component are needed the API gravity and its distillation curve. The API grades and distillation curves used to characterize feedstock, naphtha and distillates pseudo-components were obtained by a literature search and they are presented in chapter 8.

The post-processing of the results obtained from CFD simulations was done using CFD-Post, a tool from ANSYS workbench. If it was necessary an unavailable analysis, the data were exported in ASCII format and later were read using MATLAB and in MATLAB environment the treatment needed was applied..

2.2.1 Validation process

To validate the performance of the CFD simulations, experimental data in the literature were used. The validations processes were done by trying to be as accurate possible to the experimental setup, this means use the same fluids of the experimental setup, the same operating conditions and if possible the same geometry. The process validation involves three steps:

1. To propose a CFD simulation capable to describe the behavior of both phases at a particular zone.

2. To compare the results of the CFD simulation with the experimental measured data.

3. To readjust the assumptions or geometry made at the step one in the CFD simulation to accurately describe the behavior.

An iteration process between step 2 and 3 allowed to build CFD simulations to approximately describe the behavior of the phases in the experimental setups selected from literature.

2.3 Evaluation of design configurations process

The evaluation of the design configurations was done by two different methodologies, the first methodology uses the maldistribution factor proposed by Marcandelli in 2000, by this way it was possible to quantify the liquid distribution. The second way used in this work to evaluate the liquid distributions at the top of the catalyst bed obtained by CFD simulations was using a 1-D VGO-hydrocracking reactor mathematical model, by this way it was possible to estimate an approximate behavior of the performance of the reactor by solving a system of first order differential equations. The set of equations are presented in the chapter 8, it is composed by five mass balance differential equations for each pseudo-component of the reaction mechanism and the hydrogen and a differential equation for the energy balance. By using the 1-D model of the VGO-hydrocracking reactor it was only possible to obtain an approximate behavior of the reactor, however the final aim of the 1-D VGO-hydrocracking reactor mathematical model is to relate the performance of the reactor to hydrodynamic variables at the top of the catalyst bed (like velocity of the phase or volume fraction of the phases).

Chapter 3

Bottleneck identification

To achieve an improvement on a system, the first step is to identify when, where and/or why the system fails. In engineering, a bottleneck is defined as any element of a system which reduces the capacity of the system below of the demanded throughput. The improvement of the performance of the HDC reactor in this work started by an identification of process limitations (bottlenecks) that could be studied by a CFD perspective.

3.1 Bottleneck to a VGO-hydrocracking process

To identify the most usual process limitation on HDC reactor operation it was necessary use firstly a bibliography search on indexed science journals, handbooks and other related literature. Atypical information sources as HDC process surveys, gray literature and online forums were used too. Process limitation are important for both academic and industrial areas so it was important take the relevant information from both sides to build ideas and concepts about current bottlenecks in HDC processes.

The previous definition of bottleneck was used with the objective to identify any element on reactor operation that could be considered as a bottleneck, the information search showed that the bottlenecks may be associated with the type of the reactor used to host the VGO-hydrocracking process. The HDC reactions are usually hosted in trickle bed reactors (TBR), in TBR operation liquid flow distribution is one of the most critical parameters to guarantee that this kind of reactor behaves near to design values, also it is known that small variation in liquid flow distribution can lead to a substantial loss in the activity of the catalyst [21, 22, 28], in normal operation liquid flow distribution in the reactor can be noticeably different from design distribution, this condition is known as flow maldistribution and is undesirable, deviation from the design flow patterns can

be caused by preferential flow path (or channeling of fluid), by recycling of fluid or by creation of stagnant regions (or dead zones) [33]. Liquid flow distribution inside the reactor is function of diameter of reactor to catalyst particle diameter, liquid and gas flow rates, physicochemical properties of the fluids, wettability, initial distribution and orientation and shape of the catalyst [10, 19, 21].

Flow maldistribution can generate several problems on TBR operation, some of them are related to the inefficient use of the catalyst [22] like losses on the performance, selectivity or catalyst stability [7] while another common issue on operation is hot spot formation [22]. These issues will lead the reactor to loss his volumetric productivity through undesired reaction rates (as coke formation on oil refining processes) or decreasing the desired reaction rates. Finally liquid distribution also has an impact over pressure drop, higher pressure drop means high long-term operating cost of TBRs.

Although liquid flow maldistribution is not an element of the system and it is more like an undesirable situation on operation, it can be considered like a bottleneck due to the kind of issues that triggers, this issues can lead to the reactor (taken system) works below demanded throughput, further this condition is closely related to process variables as was mentioned above making possible to correct the liquid flow maldistribution by CFD simulations based on process modifications.

3.2 Bottleneck implications to the CFD simulation process

This work focused on achieve an improvement of the performance in a VGO-hydrocracking reactor using CFD simulation, as was presented in the previous section the literature suggest that the liquid distribution (or maldistribution) at the top of the catalyst bed is critical parameter to the VGO-hydrocracking process to guarantee the appropriate performance of the reactor, also the state of the art showed that the flow maldistribution has been successfully simulated with CFD simulation therefore is bottleneck that is possible to be addressed by CFD simulation.

As mention previously at the introduction chapter there are two important sections on the distribution zone: (1) the *distribution tray section* and the *dispersion zone section*. As Maiti et al. [25] showed in their review work there are different gas liquid distributors that could be used on the distribution tray section, in this work it was chose to work with a Vapor Lift Distributor (VLD) unit, this kind of distributor had not yet been simulated at the time of this thesis in the open literature.

It was concluded that there are necessary three CFD simulations to accurately describe the behavior of the phases at the distribution zone. Two simulations to describe the

VLD unit and another one to describe the dispersion zone, each of them have a chapter dedicated to explain the results obtained and how the simulation was built.

The geometry of the distribution tray and the dispersion zone was obtain by combining the information report by Bazer-Bachi et al. [31] about devices used on TBR operation to spread the liquid phase over the top of the catalyst bed and the information report by Du et al. [29] about VLD units.

In conclusion the CFD simulations done in this work will focused on appropriately describe the behavior of the phases at the **distribution zone** to improve the performance of a VGO-hydrocracking reactor.

Chapter 4

CFD simulation of gas inlet to a single VLD unit

As it was mentioned at the methodology chapter (Chapter 2) to simulate the liquid distribution at the top of the catalyst bed it is necessary to simulate the distribution tray and the dispersion zone, to describe completely both sections of the liquid distribution system three CFD simulation were built, however this chapter will focus only on the CFD simulation of the gas inlet to a single VLD unit.

The VLD unit is a U-shaped conduit device surrounded by a pool of liquid used to mix the liquid flow and the gas flow in a single stream, one of the legs (INLET leg) of the U-shaped conduit is shorter than other and have a tiny slot that is used by the gaseous phase to go inside the VLD unit, the other leg (OUTLET leg) allows the mixture stream go to the dispersion zone. Illustrative scheme of the VLD unit operation can be seen at the Figure 4.1.

Previously to this work there is no literature available about CFD simulations of VLD units and there is not clear information about how the gas phase behaves at the surroundings or at inlet slot of the VLD unit. Because of this it was necessary to simulate the behavior of the gaseous phases as approaches to the inlet slot.

4.1 CFD modeling

Like was mentioned above the VLD unit is surrounded by a pool of liquid, due to high computational resources that could be needed to simulate the pool of liquid and the interaction with the gas phase by a multiphase CFD model, it is proposed the

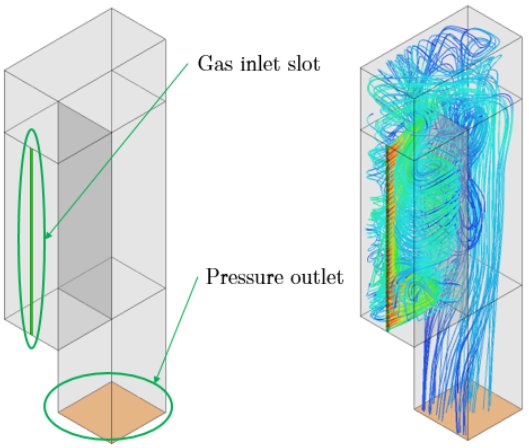

FIGURE 4.1: VLD unit operating scheme. Flow lines of the gas phase inside the VLD unit.

assumption that the liquid surface that is exposed to the gas phase acts like wall, this assumption will be examined at the result section.

A mesh with 544000 cells with a non-homogenous size distribution was used to simulate the behavior of the gaseous phase as goes to the inside of the VLD unit, the more refined section of the mesh is in front of the inlet slot to capture accurately the inlet profile. The mesh refinement can be seen at the Figure 4.2. Also a transient single phase Eulerian model on ANSYS Fluent v.15 was used until the pseudo-stationary state (PSS) was reached. It was establish that the PSS is reached using an arbitrary criteria: *the average velocity magnitude at the inlet slot of the VLD unit does not have changes greater than 5% of itself.*

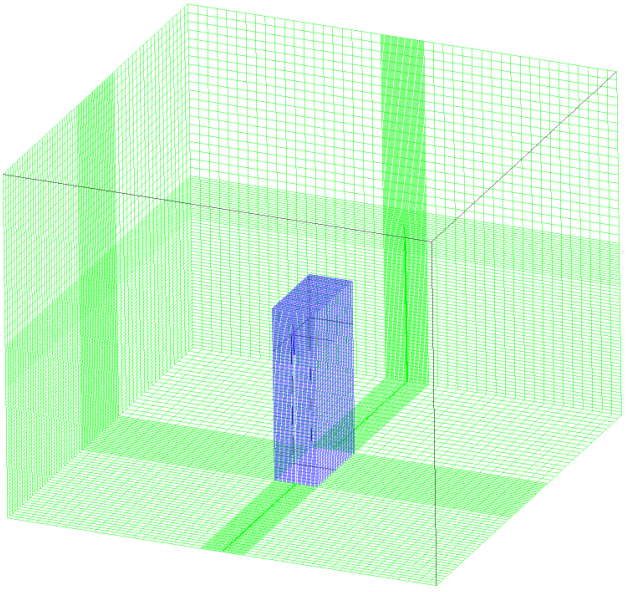

FIGURE 4.2: Mesh used in the CFD simulation of the gas inlet at the VLD unit.

To involve the turbulence effect in the simulation, principally the turbulence near at the inlet slot unit and at the interior of the VLD was chosen to use a Reynolds Averaged Navier-Stokes (RANS) turbulent model, more specifically the k-ϵ turbulent model, this kind of turbulence models offer an economic approach to compute turbulent flows providing a good level of accuracy. The k-ϵ turbulent model is a widely used model for industrial and engineering flow calculations.

4.1.1 Geometry, fluid properties, operating and boundary conditions

The geometry used in the gas inlet to a single VLD unit simulation is a cubical volume of 0.5x0.5x0.4m where the bottom surface of the cube is the liquid surface simulated like a wall, the rest of the surfaces of the cubical simulation domain (five surfaces) are inlets to the gas phase, this cubical volume simulates to be the surrounding of a single VLD unit. At the center of the cubical volume there is a parallelepiped shape with a dimensions of 0.2x0.1x0.05m and with an inlet slot of 0.002x0.15m, this parallelepiped at the center simulates to be the VLD unit. The gaseous phase use the inlet slot to goes inside the VLD unit volume in the center of the simulation domain to reach the outlet surface inside of him, for this simulation case the outlet surface was established as a pressure outlet boundary condition.

It is assumed that the gas inlet stream is pure hydrogen and there is no reactions at this point of the reactor to produce any other gas species, so the gas phase is composed only by hydrogen. As mentioned at the chapter 2 the properties of the hydrogen at the operating conditions were calculated using ASPEN HYSYS, the properties were assumed like constants because there are no great changes of pressure or temperature at the VLD unit or the surroundings. The properties used and the operating conditions are summarized in the Table 4.1.

TABLE 4.1: Gaseous phase properties on gas inlet to a single VLD unit simulation.

Properties	Value
Temperature (K)	644.15
Pressure (MPa)	17.06
Density ($kg.m^{-3}$)	6.2522
Viscosity($kg.m^{-1}.s^{-1}$)	1.5363e-05

As was mention above five surfaces are used by the gas to inlet to the simulation domain, it was choose that all of them were velocity inlets with a flat profile of 5.7 $mm.s^{-1}$, the time step used in the simulation is the 1ms.

4.2 CFD simulation results

As was mentioned at the beginning of this chapter the aim of this simulation is to capture the behavior of the gas phase as approaches to the inlet slot of the VLD unit, this objective includes the velocity profile at the inlet slot. The first step to capture behavior of the gas as goes inside the VLD unit is reach the PSS, as was said before the PSS is found by tracking the average velocity magnitude at the inlet slot. The PSS was reached after simulate $9s$ as can be seen at the Figure 4.3 at this time the tracking variable (average velocity magnitude at the inlet slot) does not change drastically. The simulation data were taken from $5s$ until the end of the simulation but only data after reached the PSS were used to built the figures shown in this chapter.

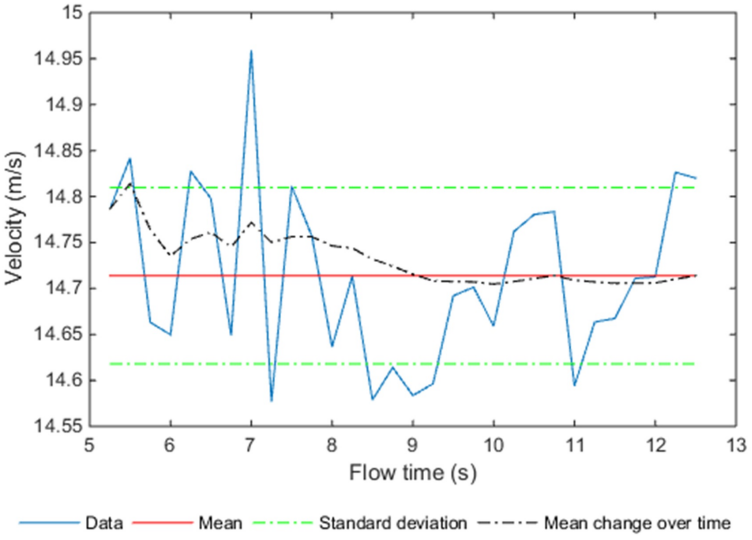

FIGURE 4.3: Tracking of the average velocity the slot inlet to idenfity when the simulation is on PSS.

As expected closer to the inlet slot higher the velocity of the gaseous phase, as can be seen at the Figure 4.4, where the horizontal axis (abscissa) is a dimensionless length that as increases it is farthest from the inlet slot. This acceleration phenomenon of the gas phase is due to the conservation of the volumetric flow. Observing the velocity profile as the gas approximates to the inlet slot in the Figure 4.4 is clear that there is a drastic acceleration of the gaseous phase near to the slot, more precisely at Ψ equal to 0.3. The Figure 4.4 also shows that the velocity remains below $2m.s^{-1}$ until Ψ is lower than 0.2, right in the vicinity of the slot.

Now that the behavior of the gas phase as approaches to the inlet slot was characterized, it seems important to known also the behavior of the phase velocity in the vertical direction to know how far the profile extends. By observing at different points of the

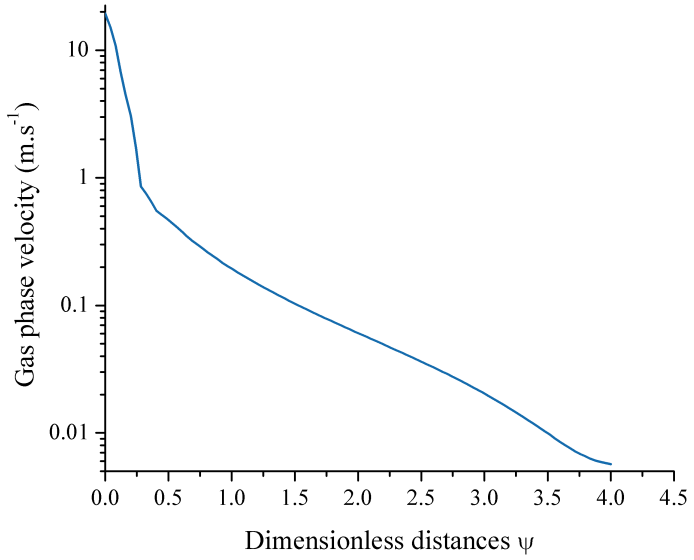

FIGURE 4.4: Behavior of the velocity magnitude. The vertical axis is logarithmic, while the horizontal axis is the ratio between X distance measured from the slot and the width of the VLD unit.

simulation domain it was concluded that the gas phase only accelerates along the inlet slot ($0 < \alpha < 1$) and along the slot this acceleration is almost uniform as can be seen at the Figure 4.5.

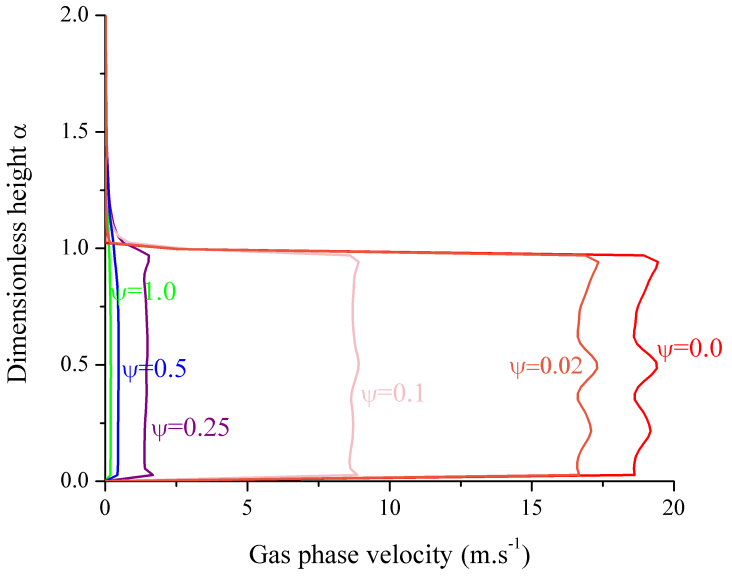

FIGURE 4.5: Velocity profile in the height direction. The dimensionless variable on the vertical axis is the ratio between the y distance and the height of the slot.

After understand the general behavior of the gas phase as goes inside the VLD, seems important to examine the assumption used at the bottom surface of the simulation domain, as was mention in this chapter this assumption was made to reduce the computational resources needed to simulate this particular section. This assumption is conceived using the concept of stratified laminar flow, in this kind of multiphase flow the velocity at the interface between the two immiscible fluids becomes equal to the velocity of the most viscous.

As it was mentioned above that the VLD unit is surrounded by a pool of liquid, it is approximately correct to assume that in real operation the liquid pool should not drastically move in a different direction that the vertical (change in the liquid level). The last assumption means the velocities in a direction different of the vertical direction if are not 0 $m.s^{-1}$ are near. At low velocities of the gas phase (like in the distant zones from the slot of the VLD unit) the interaction of the gaseous phase with the liquid pool should be low, so the interface between the fluids should behaves in a similar manner that a stratified laminar flow. Because the liquid is the most viscous fluid and practically it is stationary to any different direction that the vertical direction as was noted, the velocities at interface between the liquid and the gas phase should be near to zero.

The previous explanation will be correct only if in the simulation domain there is not large areas with high velocities, in the Figure 4.6 can be seen that this statement is true except for the area near to the slot of the VLD unit. But the area where velocity of the gas phase is above 1 $m.s^{-1}$ is not even 10% of the total liquid surface exposed to the gas phase. It was concluded that to decrease the computational resources necessary to simulate gas inlet to a single VLD unit it was approximately correct to assume that the interface between the fluids behaves like a wall with a no-slip condition as long as the area with high interaction of the gas phase over the liquid phase remains small in comparison with the total exposed area, in contrary case the assumption that the interface between fluids behaves like a stratified laminar flow is not accurate.

Finally, in the Figure 4.7 is presented the velocity profile at the inlet slot, the values presented are the velocity magnitude at the center of the 200 cells which their faces belong to the inlet slot surface. As expected, most of the variation in velocity is in the horizontal direction and as was noted before in the vertical direction the acceleration is almost uniform along the inlet slot. Also it is important to note that the horizontal axis in the Figure 4.7 is not in scale to facilitate observation of the velocity profile. This profile will be used in the next simulations as boundary condition.

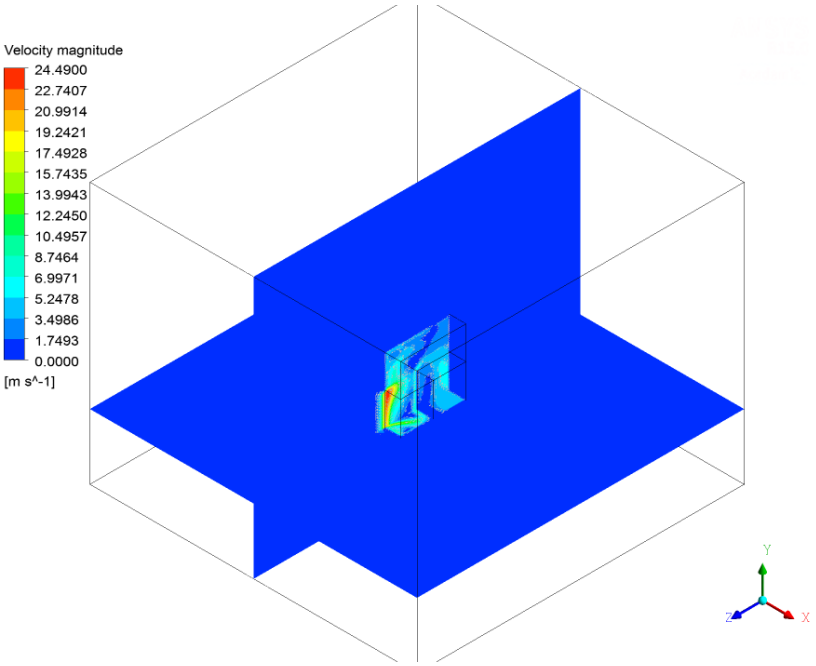

FIGURE 4.6: Velocity contours of the gas phase as goes inside the VLD unit.

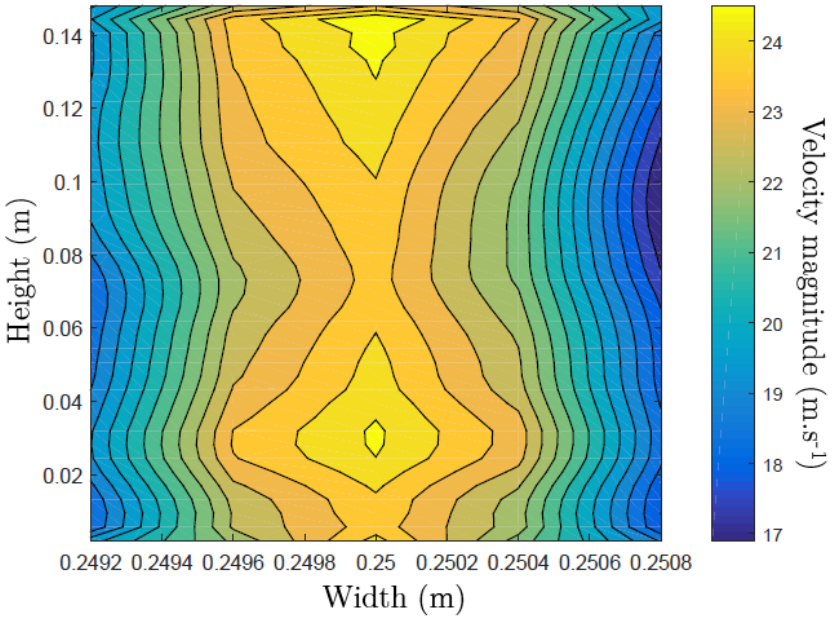

FIGURE 4.7: Velocity magnitude profile of the gaseous phase at the inlet slot profile.

Chapter 5

CFD simulation of a vapor lift distributor unit

The previous chapter focus on the behavior of the gas phase, on the other hand this chapter will change the focus to capture accurately the interaction between both phases at the VLD unit. As it was mentioned before at the VLD unit the gaseous phase flows from the outside of the VLD unit to the inside at high velocity using the inlet slot, this high velocity gas stream assists the movement of the exposed stationary liquid phase breaking its surface and lifting him through the inlet leg to the top of the VLD unit and generating a continuous flow of liquid at the outlet leg.

The literature about VLD unit at the time of this thesis is limited to some experimental papers, this research work proposes a practical way to simulate a single VLD unit using CFD, the simulation built with the methodology proposed in this chapter was validated using experimental data on literature.

5.1 CFD modeling

The CFD simulation of the VLD unit was built under the main objective to build a simulation with a low-consume of computational resources. To simulate the behavior of both phases on the VLD unit it was choose to use a multiphase transient model, specifically the Volume of Fluid (VOF) model, this model is in capacity to track the interface between two phases making possible to observe the behavior of the liquid surface exposed to the high velocity current of gas.

The main assumption of the VLD unit CFD simulation is that the only piece of the liquid pool that matters to the simulation is the portion of liquid that is right below

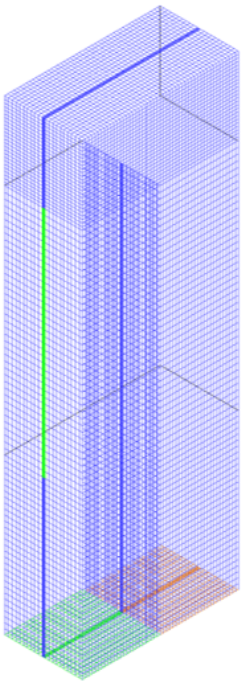

FIGURE 5.1: Mesh used in the simulation of the VLD unit with refinement in front of the inlet slot.

of the inlet leg, this liquid portion was simulated using a container with the same sizes that the inlet leg. At the bottom of the container there is velocity boundary condition that was used to guarantee that liquid height of the pool remains almost constant.

The Figure 5.1 shows the mesh used in the CFD simulation of the VLD unit, the mesh is composed by 120000 non-homogeneous size hexahedral cells, the mesh is more refined in front of the slot to capture accurately the behavior of the gas while goes inside the VLD unit. As was remarked in the previous chapter (Chapter 4)the velocity profile at the slot is inherited from the CFD simulation of gas inlet to a single VLD unit, the profile used can be seen at the Figure 4.7.

The turbulence effect on the system was model by using again the RANS k-e model, in the previous chapter (Chapter 4)was discuss the convenience of use this model on the CFD simulation, the conclusion remains, using a k-e turbulence model allows a good level of precision to predict the turbulence in the system without expensive use of computational resources.

5.1.1 Geometry, fluid properties, operating and boundary conditions

The sizes of the simulation domain are 0.05x0.1x0.3m to width, length and height, respectively. The domain is composed by two velocity inlets and one pressure outlet. An

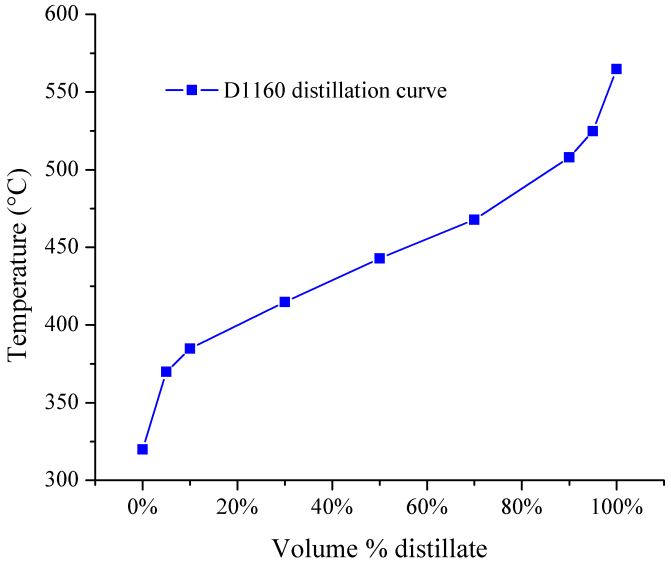

FIGURE 5.2: ASTM D1160 distillation curve for the VGO.

exclusive velocity inlet for the gaseous phase (inlet slot) with dimensions of 0.002x0.15m and an exclusive velocity inlet for the liquid phase (at the bottom of the container) that was sized as 0.05x0.05m.

In the same way as in previous chapter (Chapter 4) the properties of the liquid and gaseous phase were assumed as constants, because there is not great changes of temperature or pressure inside of the VLD unit. The properties were obtain from ASPEN HYSYS at 644.15 K and 17.0636 MPa. The gas properties remain same as in previous chapter but the properties of the liquid were calculated using the distillation curve in the Figure 5.2.

TABLE 5.1: Properties of the liquid and gas phase in the VLD unit CFD simulation.

Property	**Hydrogen (gas phase)**	**VGO (liquid phase)**
Density ($kg.m^{-3}$)	6.2522	647.6747
Viscosity ($kg.m^{-1}.s^{-1}$)	$1.5363e^{-1}$	$5.5454e^{-1}$
Surface tension ($dyn.cm^{-1}$)	6.0121	

As was noted previously there are three boundary conditions in the simulation domain, the inlet slot is a velocity inlet boundary condition used exclusively by gaseous phase, where the velocity values on each cell were inherited from the previous simulation, Figure 4.7. At the bottom surface of the container, it is a velocity inlet boundary condition to the liquid, a flat profile (constant entrance velocity) was used instead. The container was patched with a starting pool of liquid with a height of 0.1m and the velocity inlet boundary condition restores the liquid that goes out at a rate of 0.2244 $m.s^{-1}$.

5.2 Validation process

A validation process was done to ensure that the models and the assumptions used in the CFD simulation represent correctly the behavior of the phases at the VLD unit. At the time of this thesis there is no standard procedure to validate a CFD simulation of a VLD unit. Instead it was proposed to validate the results of the VLD unit CFD simulation using the pressure drop between two points inside simulation domain, the chosen point were the gas inlet slot and the outlet. The data used in the validation process was the experimental pressure drop data obtained by Nolin [30] for the water/air system. As not all the dimensions were available, initially the opening between the inlet and outlet leg was used as parameter and later was used the area of the inlet slot.

Initially was assumed that the liquid phase has a volume fraction so low (below 0.1) that is possible to capture the pressure drop at the VLD only simulating the gaseous phase. Using the opening between the inlet and outlet leg as parameter in the simulations three simulation were proposed:

- Opening length between the inlet and outlet leg equal to $2.5cm$.
- Opening length between the inlet and outlet leg equal to $5cm$.
- Opening length between the inlet and outlet leg equal to $15cm$.

The results at the Figure 5.3 show that this assumption is not correct, for the case where the opening between legs have a length of $15cm$ the pressure drop is under predicted to any volumetric gas flow. To the cases where opening between legs have a length of 5 and $2.5cm$ the pressure drop to the lowest values of volumetric gas flow were under predicted too, but to the highest volume gas flow rate the pressure drop was approximately captured. These results show that the assumption of neglect the presence of liquid is correct only to high volumetric gas flows. Also it was noted that the case with an opening between legs equal to $15cm$ under predicted the values of pressure drop for all volume gas flow rates but capture better the tendency of the experimental data.

The previous set of simulations allowed to identify the importance of the liquid phase to validate the VLD unit simulation. Then another set of simulations were proposed using an opening between the legs of $15cm$, but the liquid phase increased the computational cost of the CFD simulations, in order to complete the validation process only the points at the ends ($65\ m^3/h$ and $140\ m^3/h$) were simulated. In the first set of simulations (using an inlet slot area of $3cm^2$) the pressure drop was overestimated as can bee see at the Figure 5.4. As was noted previous in this section some dimensions of the experimental

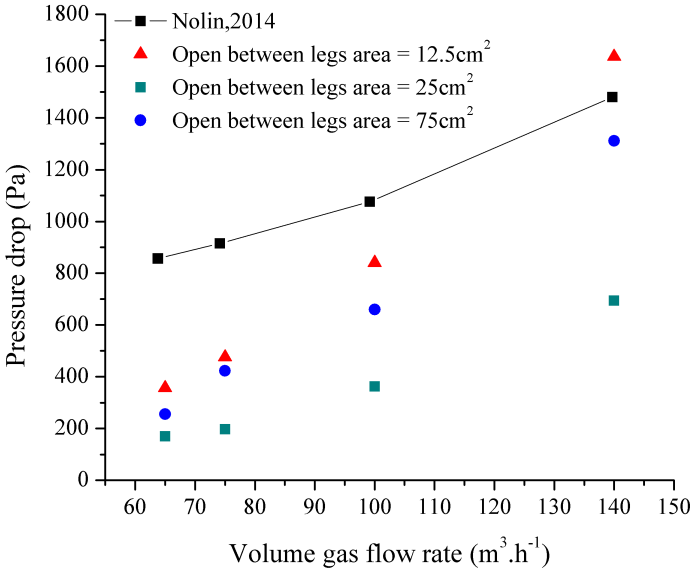

FIGURE 5.3: CFD simulation of the gas phase to validate the pressure drop on the VLD unit.

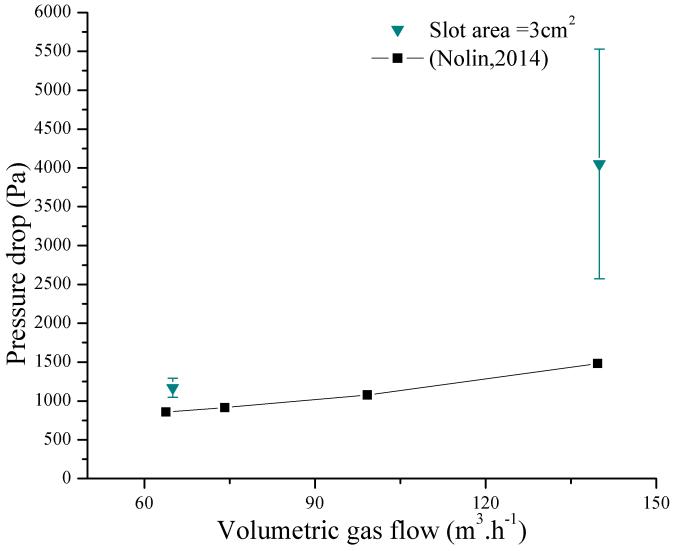

FIGURE 5.4: Comparison between the data measured by Nolin and the CFD simulation results when the inlet slot area is equal to $3cm^2$

setup were unavailable, to capture accurately the pressure drop measured by Nolin a parameter modification of the geometry of the simulation was done using the area of the slot as parameter.

Two other cases were evaluated, an inlet slot area of $6cm^2$ and $10.5cm^2$ were used, it was presumed that a bigger inlet slot area will reduce the velocity at the inlet slot and also

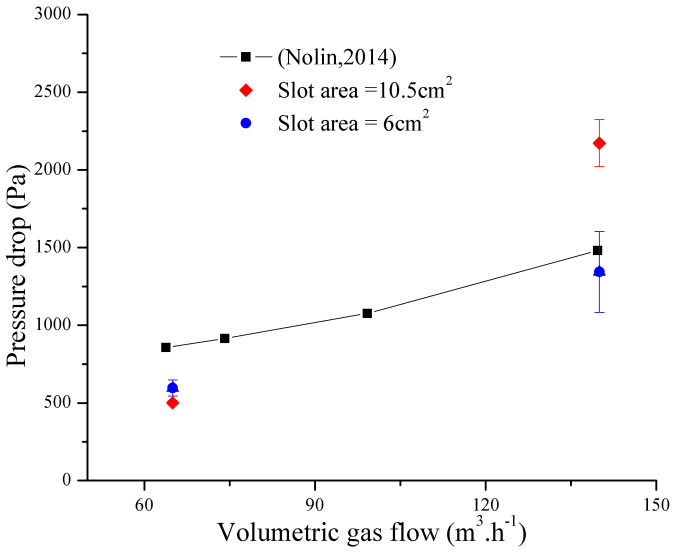

FIGURE 5.5: Comparison between the data measured by Nolin and the CFD simulation results when the inlet slot area is varied.

reduce the pressure drop at the VLD unit. Both simulations showed that the hypothesis proposed previously is fulfilled as can be observe at Figure 5.5, if the area of the inlet slot increases, the pressure drop at the VLD unit declines drastically as can be concluded by comparing the results of the simulation with bigger slot area (inlet slot area of $6cm^2$ and $10.5cm^2$) against the first VOF simulations (inlet slot area of $3cm^2$).

By comparing the predicted results by CFD simulation with the experimental data measured by Nolin it is possible to state that the CFD simulations proposed and the models used on them can represent the behavior of the phases inside a VLD unit. In addition to the tendency of the pressure drop (which was predicted by all the simulations), it was possible to predict the values of the pressure drop obtained from the experiments however the geometry of the VLD unit is a key parameter to achieve better and more accurate simulations.

5.3 CFD simulation results

To capture the behavior of the phases at the VLD unit a transient VOF model was used, when transient formulation of the models are used previously to obtain the results of the simulation achieve the PSS is needed. In particular to the VLD unit simulation the PSS was obtained by tracking the average volume fraction of the liquid and the velocity at the outlet of the VLD unit. The data is presented in this section is taken after the PSS is reached.

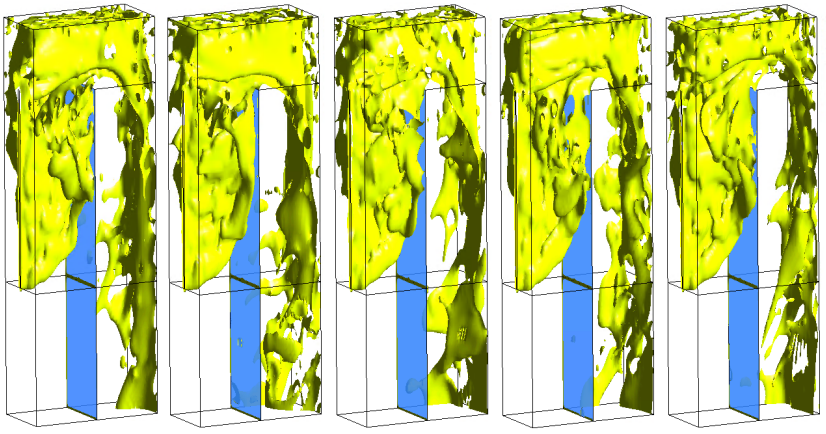

FIGURE 5.6: Iso-surface of liquid phase volume fraction at different times.

The first step in the flow analysis inside the VLD unit was done by examining an iso-surface for a liquid-phase volume fraction, an iso-surface is a surface that represents points of constant value within a volume of space. The iso-surface was calculated using CFD-post with a liquid volume fraction of 0.75, the change over time of the iso-surface after the PSS can be observe in the Figure 5.6. The iso-surface showed three important results:

- At the inlet leg there is a large portion of the simulation domain where the volume fraction of the liquid phase is above 0.75, this zone with high liquid concentration explains why the simulations done at validation process needed of multiphase models instead of single phase formulation, the initial assumption where the gas phase is in a higher concentration than the liquid phase is not satisfied at the inlet leg, the pressure drop generated by the high liquid concentration at the inlet leg only could be observed after using multiphase models.

- The interaction between the high velocity gas phase with the stationary liquid phase at the inlet leg creates a continuous flow of liquid. Inside the VLD unit the behavior of the phases is similar to a wispy-annular flow, in this kind of flow one of the phases moves in contact with the wall and the other moves in the center of the pipeline, this multiphase flow behavior change when the mixture reaches the outlet leg.

- At the outlet leg a particular behavior was found by the flow analysis, a significant portion of the liquid phase descents in contact with the opposite wall of the gas entrance, Du et al. [29] in 2014 experimentally evidenced this behavior to the water/air system at standard conditions, even if the conditions and fluids are different this similar behavior between the experimental and simulation data brings more confidence of the simulation results.

Once that was obtain a qualitative behavior of the phases inside the VLD unit using the iso-surface, it was necessary a quantitative analysis, this analysis starts with building the liquid volume fraction profile along the VLD unit. This profile was built using planes at different heights at each of the legs of the VLD unit, 15 points were taken, 5 at the inlet leg and 10 at the outlet leg. In the Figure 5.7 is possible to seen how the volume fraction of the liquid phase decreases from a value of almost 1 near to the surface of the liquid pool to a value less than 0.1 at the outlet of the VLD unit. It is clear that as larger β smaller the volume fraction of the liquid. This behavior of the liquid phase is due to exchange of momentum between phases, the high velocity gas stream loses momentum that translates into a velocity decrease with a rise of volume fraction, instead the behavior of liquid phase is the complete opposite, using the momentum exchanged with the gas phase the liquid phase accelerates and decreases his volume fraction.

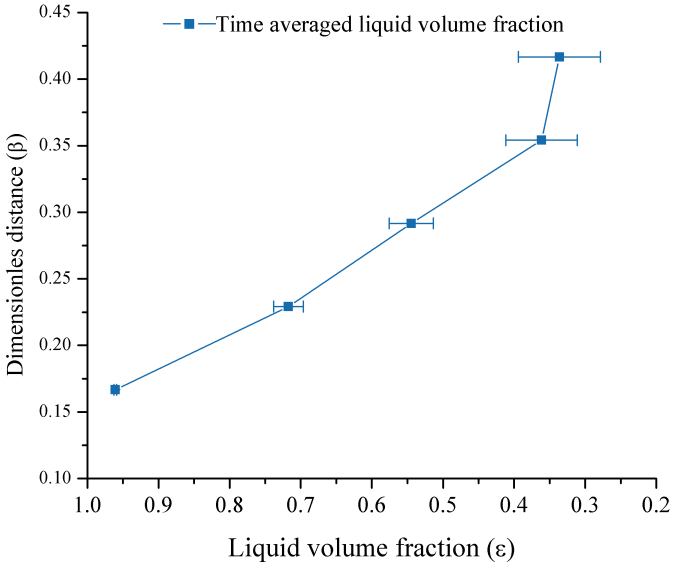

FIGURE 5.7: VLD unit liquid phase volume fraction profile along the inlet leg.

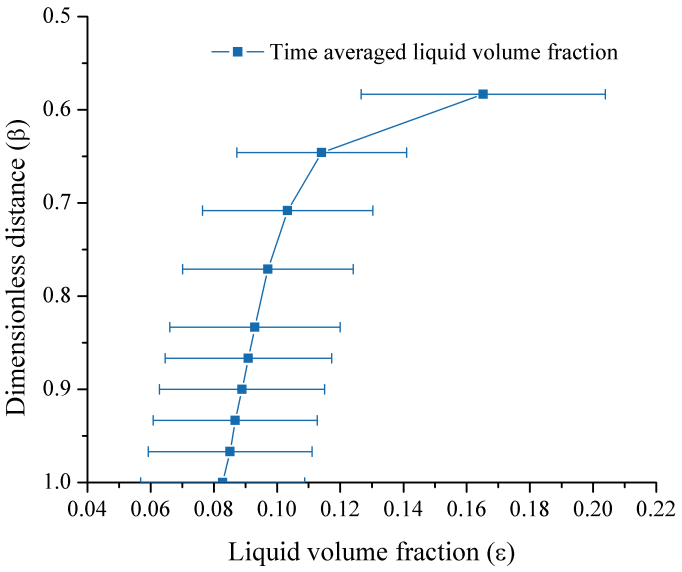

FIGURE 5.8: VLD unit liquid phase volume fraction profile along the outlet leg.

Chapter 6

CFD simulation of the dispersion zone

Like it was mentioned at the chapter 3 to simulate the liquid distribution at the top of the catalyst bed it was necessary to simulate the distribution tray and the dispersion zone, the past two chapters described a single VLD unit using two CFD simulations, on the other hand this chapter will focus on the simulation of the dispersion zone. This simulation is the final step and yields the liquid distribution at the top of the catalyst bed.

The dispersion zone is a catalyst-free volume located between the distribution tray and the catalyst bed to guarantee dispersion of the liquid/gas mixture that exits from the VLD units. The mixture stream exiting at high velocity from the VLD unit reduces his velocity as moves from the outlet of the VLD to the top of the catalyst bed. Similar to the behavior of a jet stream, the flow velocity decreases as moves away from flow center and the width of the stream flow increase as the stream goes from the outlet of the VLD to the top of the catalyst bed. This behavior increases the spread of the liquid over the catalyst bed but the collision of the flow with the porous bed also influences the liquid distribution.

6.1 CFD modeling

As it was mention previously the dispersion zone is free of catalyst, in the cubical simulation domain used to simulate the dispersion zone there are a free-catalyst simulation zone and a porous simulation zone. The porous zone was used to simulate the top of the catalyst bed. It was chosen not simulate all the distribution tray, instead simulate

a square arrangement of four VLD distributors with four symmetry boundary conditions in the vertical surfaces of the cubical domain, by replicating the profile with the symmetry boundary conditions a larger area can be obtained if it is needed, using this configuration it was possible to study if there is an interaction between injectors in any direction without an excessive use of computational resources. To properly export the velocity and volume fraction from the previous simulation four velocity inlets were used, also by this way was possible to manipulate independently each velocity inlet allowing to evaluate if the alignment of the VLD units could enhance the liquid distribution at the top of the bed. Finally a pressure outlet boundary condition was used at the bottom surface of the simulation domain.

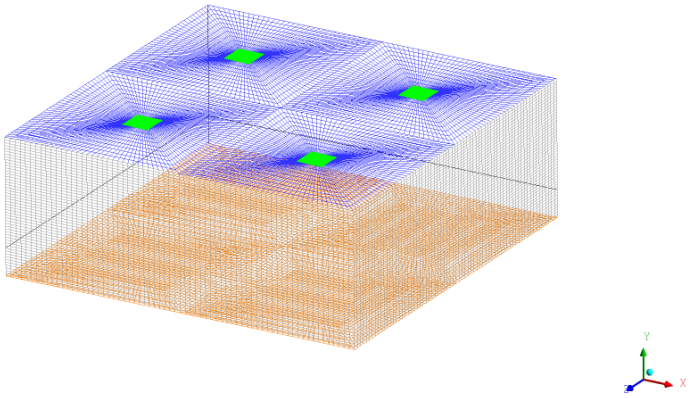

FIGURE 6.1: 500k non-homogeneous hexahedral cells mesh of the dispersion zone.

The mesh used on the simulations of the dispersion zone has 500000 non-homogeneous hexahedral cells, the velocity inlets have a high refinement to accurately capture behavior of the mixture stream as moves away from the boundary conditions in the simulation domain as can be seen in the Figure 6.1. The CFD simulation of the dispersion zone was built in ANSYS Fluent v.15 using the Eulerian-Eulerian multiphase model in transient form with a time step of $1ms$. In this simulation the turbulence model used was the RANS k- model that allow to capture accurately the turbulence generated by the collision of the streams with the top of the catalyst bed.

6.1.1 Geometry, fluid properties, operating and boundary conditions

The cubical domain is sized by 0.674x0.674x0.25m, the dimensions were calculated using the cross sectional area of the reactor and the number of injectors needed to guarantee the liquid flow reported by Mohanty [32]. Using 100 injectors guarantee the liquid flow reported and also the gas phase opening rate defined by Du et al. [29] it is kept in the

suggested range. The free-catalyst simulation zone have a depth of $0.2m$ and porous simulation zone that is right below uses the rest of length.

The same operating conditions of the VLD unit simulation were used on this one, as can be observe at the CFD simulation of a VDL unit chapter (chapter 5) the pressure drop in the VLD unit is negligible when is compared against the total pressure of the reactor. The temperature also remains constant because there is no sources or sink of heat in the process, besides the reactor was assumed like adiabatic, a typical operational condition to this kind of reactor. Due to there is no great changes of pressure or temperature on the system same properties in the Table 5.1 were used.

As mention above the top of the catalyst bed was simulated using an ANSYS Fluent v.15 porous zone, the bed properties used were calculated using mean values of volume fraction of the phases (0.35 and 0.03 to the gas and to the liquid respectively) and the interaction between phases model proposed by Attou et al. [14], the values obtained can be seen at the Table 6.1.

TABLE 6.1: Properties used on the porous zone in the simulation domain.

Property	**Liquid phase**	**Gas phase**
Viscous Resistance Coefficient (m^{-2})	1.7765e+09	1.6910e+08
Inertial Resistance Coefficient (m^{-1})	5922.7	949.04

In the four velocity inlet boundary conditions at the top of the simulation domain a velocity profile and liquid volume fraction profile were used, as it was mention along the document this profiles are inherited from the previous simulation (VLD unit CFD simulation in the chapter 5), the liquid volume fraction profile and velocity profile were taken at certain time after the PSS was reached. In the Figure 6.2 and 6.3 the liquid volume fraction profile and the velocity profile of the phases can be seen, respectively.

6.2 Validation process

The dispersion zone CFD simulation was validated employing the liquid distribution measured by Du et al. beneath the distributor using liquid collectors at a certain distance not reported. Air and water were used as gas and liquid phases, respectively, just like Du et al did in their own experimental setup.

The dispersion zone simulation domain was built using the dimensions reported for collectors in the experimental setup of Du et al., eleven collectors were used with a width of $0.04m$, with a total length of $0.44m$. Because the separation between the collectors and the distributor was not reported like was mention previously the depth

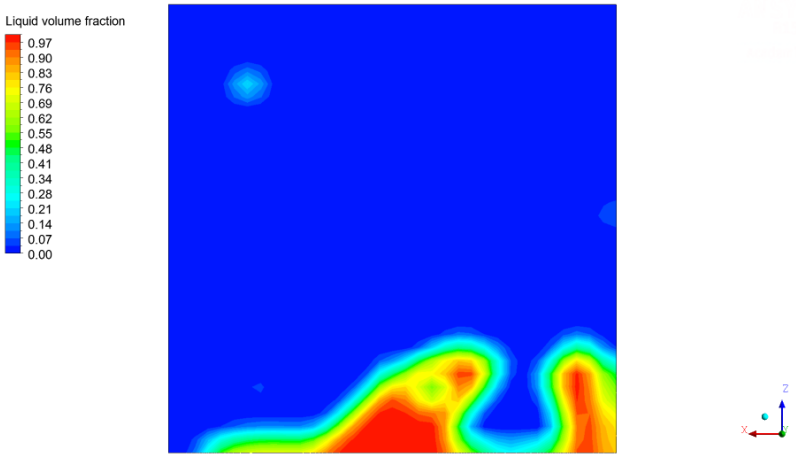

FIGURE 6.2: Liquid volume fraction profile at the velocity inlets in the dispersion zone CFD simulation.

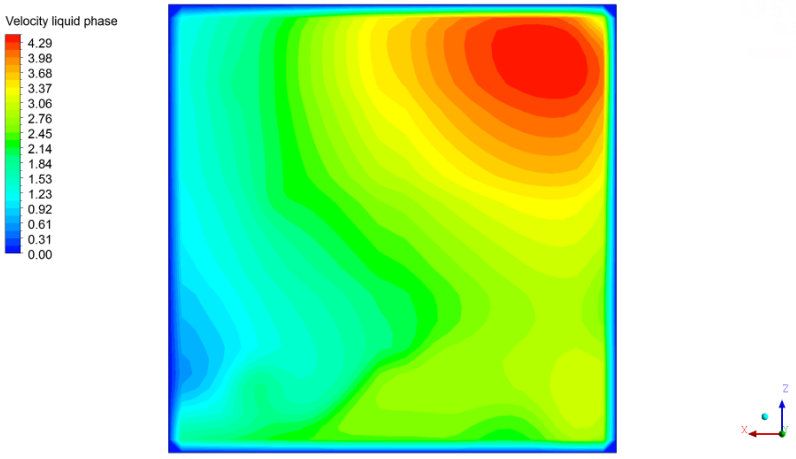

FIGURE 6.3: Velocity profile at the velocity inlets in the dispersion zone CFD simulation.

of the simulation domain was assumed as $0.4m$. The dimensions of the dispersion zone simulation domain used to the validation process were 0.44x0.44x0.4m.

The description of the experimental setup built by Du et al. refers to a single distributor, which was represented in the CFD simulation of the dipersion zone by velocity inlet boundary condition, the velocity and volume fraction profiles used in the inlet boundary condition were obtained from a CFD simulation of a VLD unit using the same flow velocities to the gas and liquid phase ($0.044m/s$ to the liquid phase and $4.4m/s$ to the gas phase) in the inlet boundary conditions, unfortunately the dimensions of the VLD unit were assumed as they were not reported by Du et al.

To simulate the liquid collectors of the experimental setup eleven surface monitors for liquid volume flow were used, each of them with a same area as a single collector ($0.0016m^2$).

The Figure 6.4 shows the CFD simulation results against the experimental data measured by Du et al., a rough representation of the experimental data was obtained but the experimental data trend was approximately captured. There are two differences between the CFD simulation results and the experimental data:

1. The experimental data have bigger values of flow to the bins next to the peak but lower values to farthest bins, the CFD simulation have a porous zone at the outlet to bring converge to the CFD simulation and to avoid reverse flow at the pressure outlet of the simulation domain, even if this configuration is more similar to the real operation of the VLD unit this porous zone could displace a portion of the liquid flow to the farthest bins from the bin peak.

2. The value of the peak was approximately captured by the CFD simulation but the location did not, the location of the VLD unit and the portion of the liquid descending in contact with the wall that is typical of the VLD unit operation could displace the location of the peak. The liquid descending in contact with the wall portion is so high that miss place the VLD unit easily displace the peak of the CFD data.

A rough capture of the experimental data trend was obtained by the CFD simulation but it is important to note that several assumptions were made during the validation process also the fact that the velocity of the phases were reported instead on the volumetric flows difficult the process validation. Even if a refinement of the CFD simulation is needed, to obtain a better representation of the experimental data than actually obtained a better description of the experimental setup is needed.

6.3 CFD simulation results

The dispersion zone CFD simulation allows to capture the liquid distribution at the top of the catalyst bed, as was established at the chapter 2, the first step to simulate the dispersion zone by a CFD transient simulation is to reach the PSS, similar to the previous CFD simulations the PSS was tracked by following the evolution of a simulation variable, to this particular case the *liquid volume fraction* at the top of the catalyst bed, after $12s$ the tracked variable seems not have important changes of itself, so it was settled that the PSS was reached. After achieve the PSS, an analysis of the phases behavior in the simulation domain was done, each zone in the simulation domain (free-catalyst zone and porous zone) was examined separately, first the free-catalyst zone and later the porous zone.

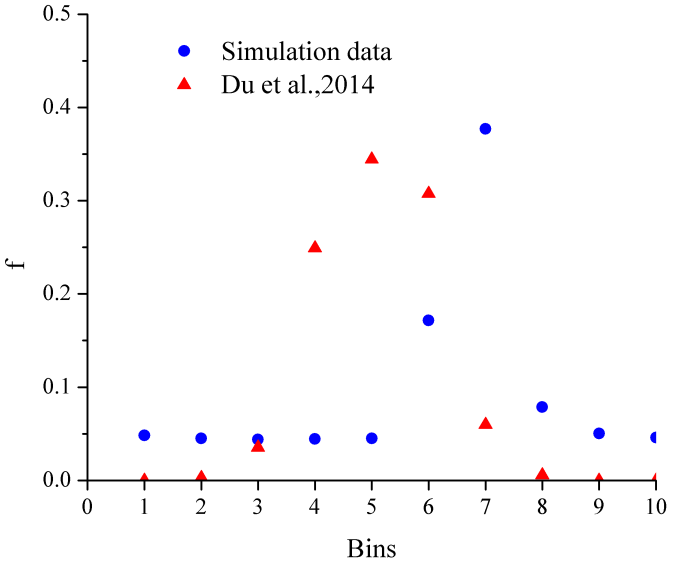

FIGURE 6.4: Comparison between experimental data measured by Du et al., 2014 and calculated data.

The average liquid volume fraction at the top of the catalyst bed (0.1282) is higher than the liquid volume fraction at the inlets (0.0888), this change in the liquid volume fraction suggests that in the free-catalyst zone there is a liquid concentration phenomenon. In the Figure 6.5 can be seen that the liquid is concentrating as goes from the outlet of the VLD unit to the top of the catalyst bed. To explain this behavior is important to note that there are two different zones in the inlets as can be seen at the Figure 6.2, a high liquid concentration zone and a low liquid concentration zone, the streamlines analysis at the inlets indicates that the path follow by the mixture going out from the zone with low liquid concentration is larger than mixture that goes out from the zone with high concentration of liquid, this behavior can be seen at the Figure 6.6. This means that mixture with low liquid concentration tends to go directly to the upper part of the dispersion zone allowing that liquid phase concentrates just above the top of the catalyst bed. The described behavior of the entering mixture illustrates why the liquid volume fraction growths as the depth of the simulation domain increases.

The analysis of the porous zone begins with the presentation of the distribution of liquid phase over the top of the catalyst bed by a contour of the liquid volume fraction (Figure 6.7), at first sight it is clear that there are zones with high and low concentration and this zones are associated with the velocity inlet boundary conditions.

At the Figure 6.7 is possible to see how the distribution of the liquid phase in the top of the catalyst bed is highly dependent of the liquid distribution at the outlet of the VLD unit. Also can be noted that the point of higher liquid phase concentration is displaced

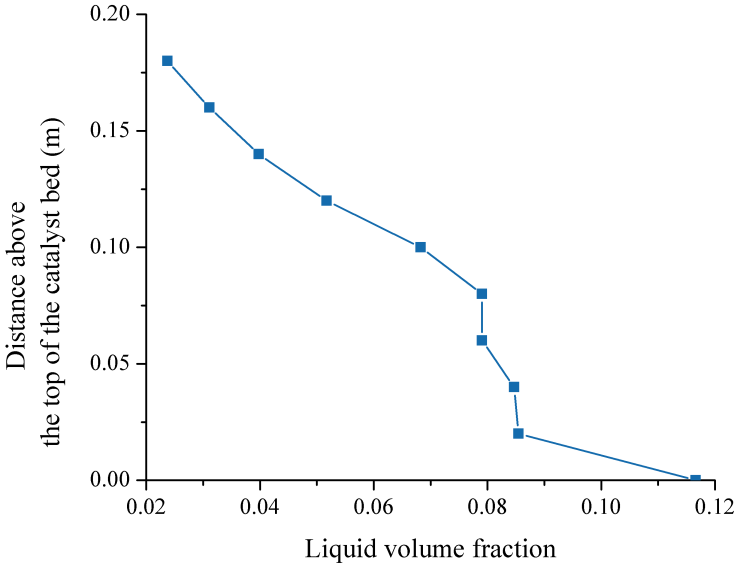

FIGURE 6.5: Liquid volume fraction profile above the top of the catalyst bed.

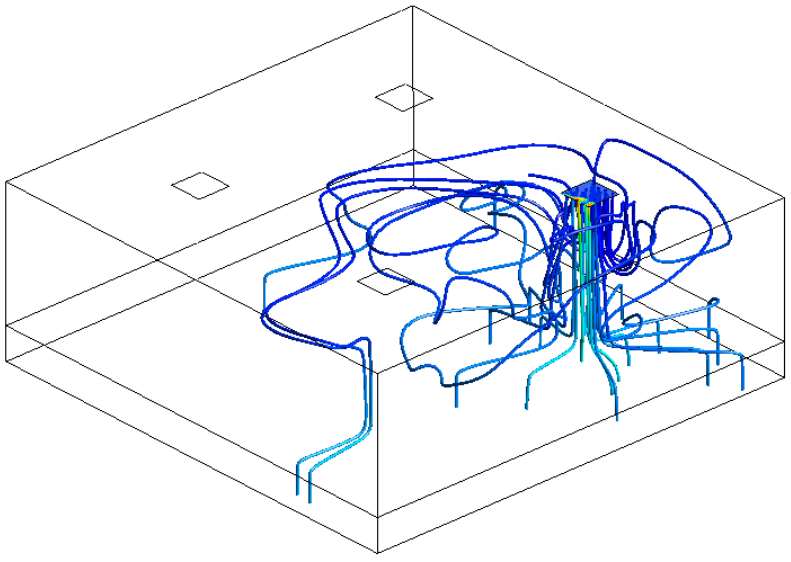

FIGURE 6.6: Stream lines from the velocity inlet boundary condition colored by the liquid volume fraction of the liquid phase.

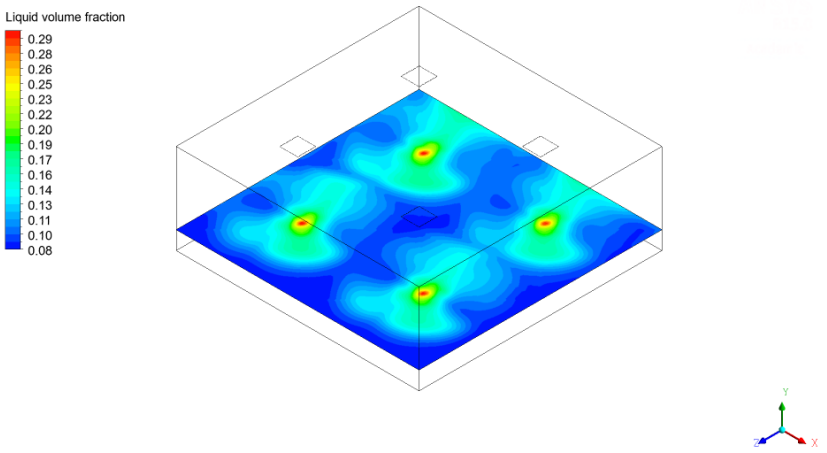

FIGURE 6.7: Liquid volume fraction distribution over the top of the catalyst bed.

towards zone with higher concentration of liquid in the outlet of the VLD unit, this means that the liquid descending in contact with wall in the VLD unit have a significant effect on the liquid distribution at the top of the catalyst bed.

Three liquid volume fraction profiles at different points inside the porous zone of the simulation domain were obtained and are presented in the Figures 6.7, 6.8 and 6.9. The Figures show the slight expansion of the liquid phase high concentration zone while the catalyst bed depth increases, this behavior agrees with previous data found in literature where it is settled that the liquid distribution is function of the depth in the reactor [21], thereby the liquid distribution is enhanced as moves from the top of the catalyst bed to the outlet surface.

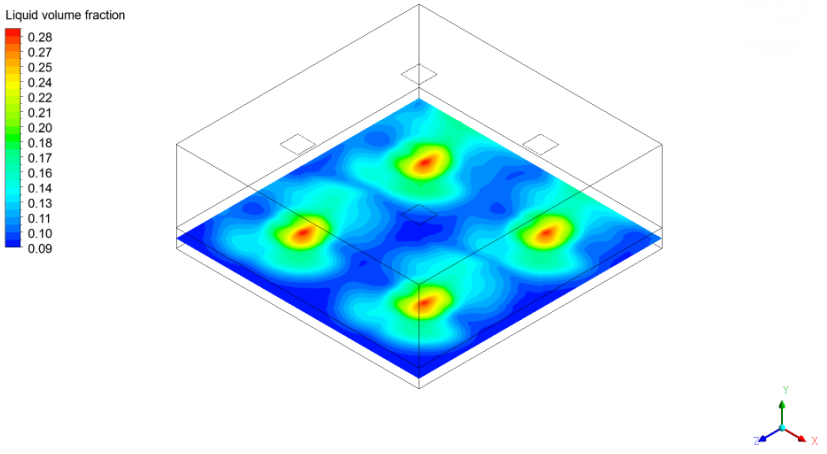

FIGURE 6.8: Liquid volume fraction distribution 2.5 *cm* below the top of the catalyst bed.

The variation of the liquid volume fraction when the surface moves away from the top of the catalyst bed implies that the velocity is changing as well, as can be seen in the

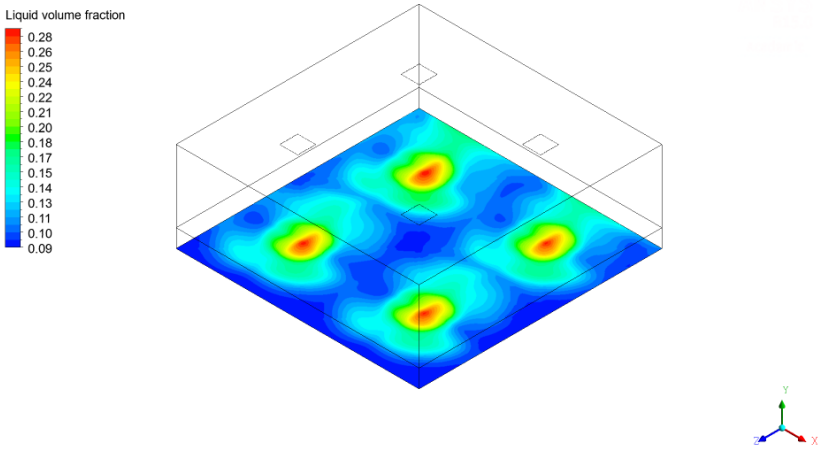

FIGURE 6.9: Liquid volume fraction distribution 5 *cm* below the top of the catalyst bed.

Figures 6.10, 6.11 and 6.12, there is an extreme variation of the velocity right after the flow passes the top of the catalyst bed, the same location as the liquid volume fraction changes.

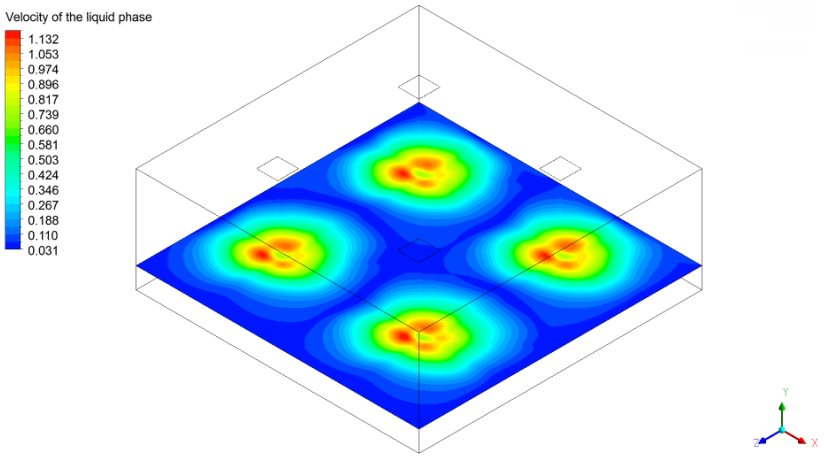

FIGURE 6.10: Contour of the superficial velocity magnitude of the liquid phase in $m.s^{-1}$, over the top of the catalyst bed.

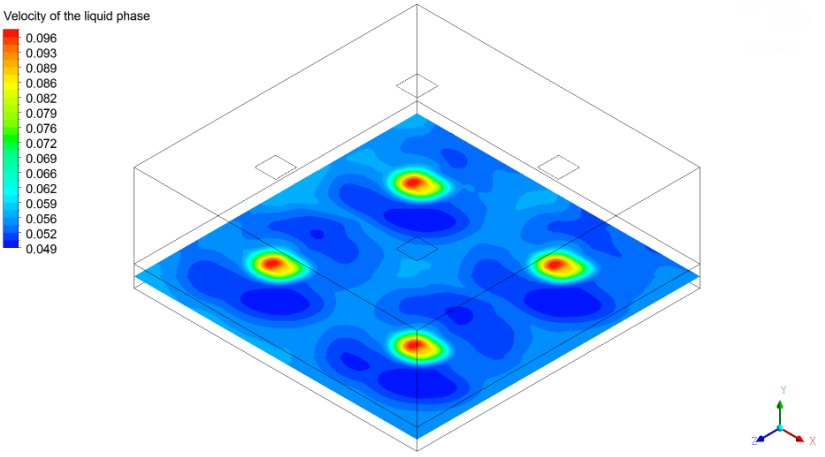

FIGURE 6.11: Contour of the superficial velocity magnitude of the liquid phase in $m.s^{-1}$, $2.5cm$ below the top of the catalyst bed.

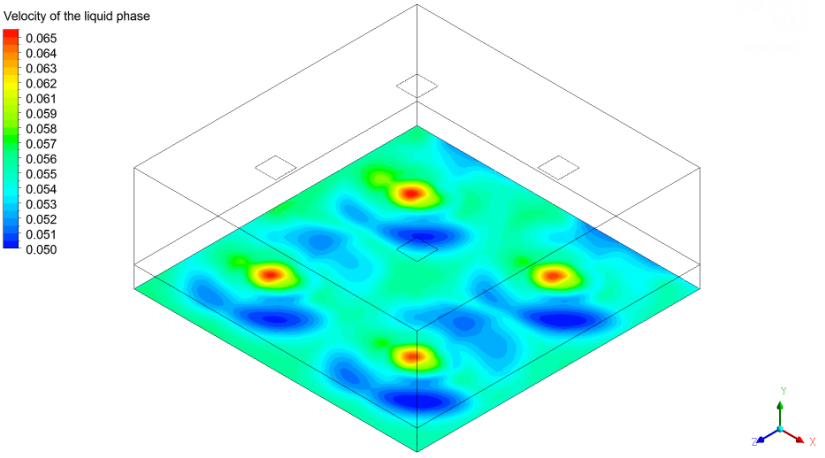

FIGURE 6.12: Contour of the superficial velocity magnitude of the liquid phase in $m.s^{-1}$, $5cm$ below the top of the catalyst bed.

Chapter 7

Parameter variation processes to enhance the liquid distribution

This chapter explains the parameter variation process done over the geometry of the VLD unit and the dispersion to enhance the liquid distribution. In the VLD unit section, the height of separator plate between the legs was varied to eliminate the liquid phase flow in contact with the wall, the process shows that using height of separator plate only can minimize the problem but is not complete solved, future work will focused in propose new variation over the geometry to obtain a better distribution. At the dispersion zone section, Du et al. suggested that the separation between the distribution tray and the top of the catalyst bed can enhance the liquid distribution, when the length is duplicated the statement proposed by Du et al. is correct, future work will consider if the there is a limit to extend the separation between the distribution tray and the top of the catalyst bed.

7.1 Parameter variation process over the VLD unit

The liquid phase flow in contact with the wall is a recurring problem in VLD unit operation, this problem has been identified experimentally (as was mentioned previously Du et al. report a similar phenomenon) and by CFD simulation (as can be seen at the chapter 5), a parameter modification over the geometry of the VLD unit was done trying to reduce this phenomenon, as was noted in chapter 6 liquid phase flow in contact with the wall phenomenon is closed related with some liquid distribution issues at the top of the catalyst bed.

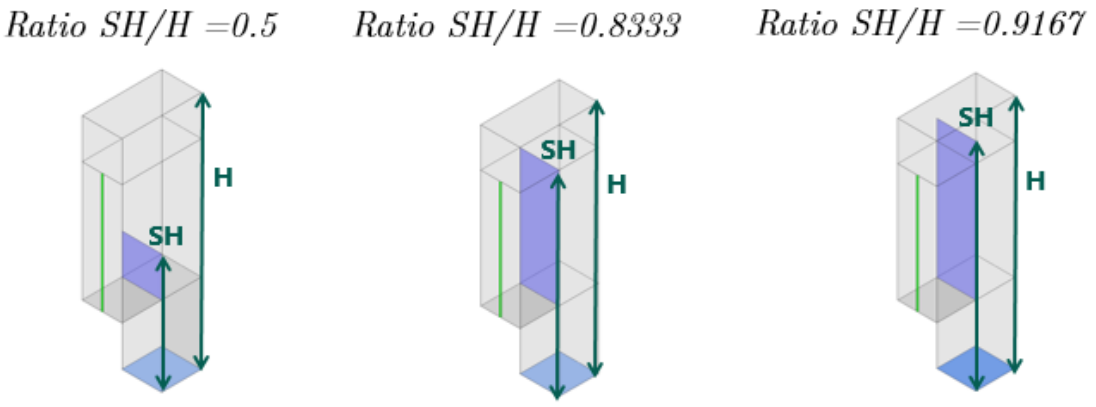

FIGURE 7.1: Geometry changes done by change the ratio of separator wall height (SH) to total VLD unit height (H)

The openning between legs characteristic length was modified by varying the ratio of separator wall height (SH) to total VLD unit height (H). Three different ratios were used: 0.5, 0.84 and 0.92 and the liquid distribution at the exit of the VLD unit was studied, each of the changes done over the geometry of the VLD unit can be observe in the Figure 7.1. The ratio of separator wall height (SH) to total VLD unit height (H) was selected for this parameter modification process because was found to have a significant effect over the behavior of liquid phase and the liquid distribution inside the VLD unit.

The liquid distribution at the outlet of the VLD unit was studied using the maldistribution factor (M_f) analysis, this strategy was extensively explain at the theoretical framework in the chapter 1. The Figure 7.2 shows a comparison of the liquid distribution in the outlet surface of the VLD unit among the three cases studied, all the studied cases showed the same zone with high concentration of liquid flow in the wall opposite to the gas entrance. Then, the modification characteristic length of the opening between legs can reduce but cannot eliminate the phenomenon of liquid phase flow in contact with the wall. The Table 7.1 shows the maldistribution factors obtained for each case, based on the calculated coefficients the best liquid distribution is yielded when a ratio of separator wall height (SH) to total VLD unit height (H) equal to 0.86 was used. The comparison of the liquid distribution in the nine partitions (Figure) yields to the same conclusion.

TABLE 7.1: Change of the Maldistribution factor at the outlet of the VLD unit when the ratio of separator wall (SH/H) changes over time.

The ratio of separator wall (SH/H)	Maldistribution factor (M_f)
0.50	0.59
0.84	0.38
0.92	0.40

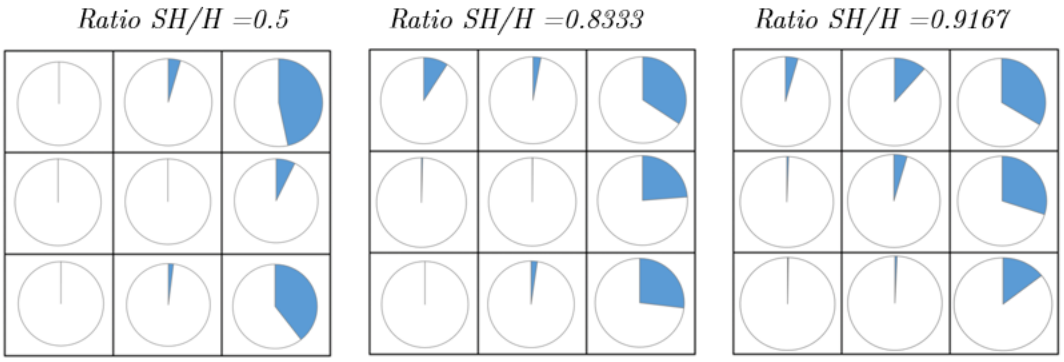

FIGURE 7.2: Comparison of the liquid distribution at the outlet of the VLD unit through nine partitions when the ratio of separator wall (SH/H) changes over time.

7.2 Parameter variation process over the dispersion zone

Du et al. suggest that the separation between the distributor and the top of the bed influences the dispersion of the liquid over the surface, using the CFD simulation built to the dispersion zone the depth of simulation domain was increased (from 20cm to 40 cm), to examine how the variation of the length between those points affects the liquid distribution. The liquid volume fraction distribution at the top of the catalyst bed is presented for both cases in the Figures 7.3 and 7.4, at first sight is possible note that the liquid distribution to the case with larger depth have a more homogeneous contour than the opposite case, both cases were examined with the same strategies (maldistribution factor M_f and liquid flow distribution) used along this document to verify if the statement previously stated is correct.

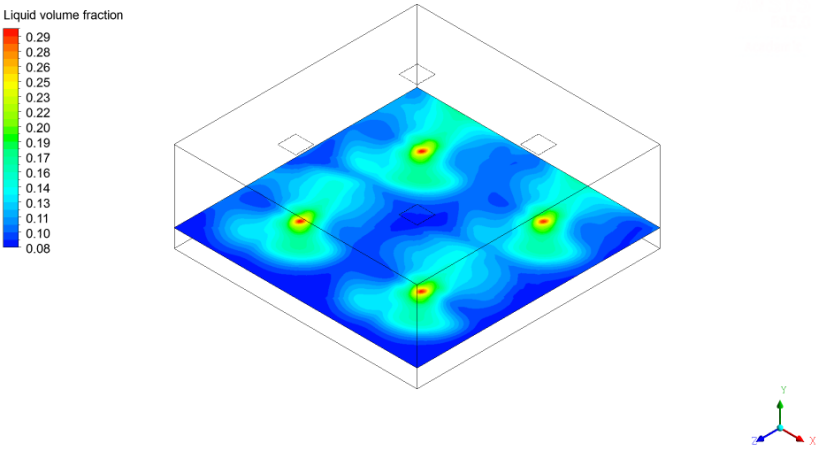

FIGURE 7.3: Liquid volume fraction distribution over the top of the catalyst bed, simulation with a depth of 20cm.

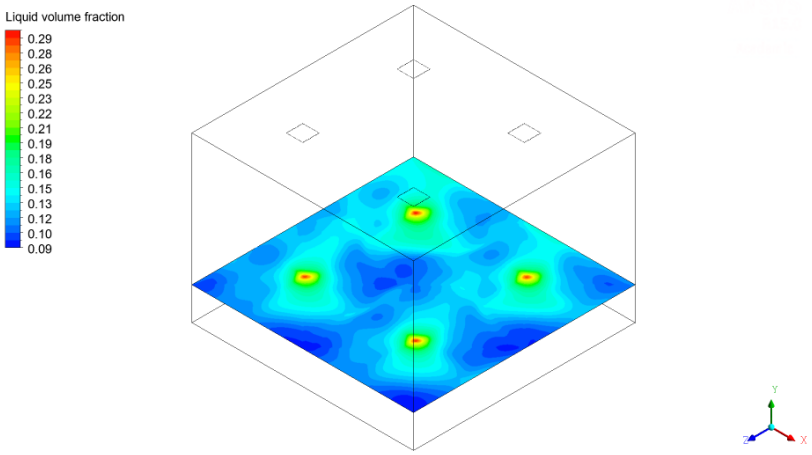

FIGURE 7.4: Liquid volume fraction distribution over the top of the catalyst bed, simulation with a depth of 40cm.

An analysis using the liquid maldistribution factor M_f shows that increasing the depth of the simulation domain it was possible to decrease the maldistribution factor (from 0.1642 to 0.0746). In the Figures 7.5 and 7.6 can be seen that the liquid flow at the center slightly increases in the case with larger depth, another important fact to be noted is that the corner zones have the larger flows, this happens because the velocity inlets are located just above, but the dispersion zone configuration with a larger depth increases slightly the flow in the center of the simulation domain.

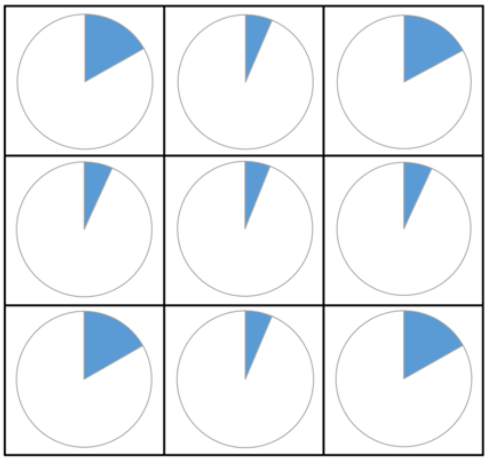

FIGURE 7.5: Liquid flow distribution in 9 planes at the top of the catalyst bed to the simulation domain with 20cm of depth.

Different comparisons between both simulations were done (streamlines analysis), but there were no significant difference among the behaviors of both simulations. At the Figure 7.7 can be observed that the behavior of the flow velocity along the depth of the dispersion zone, the behavior is significantly different to same location, both simulations starts with the same velocity but the transition is smoother for the case with a larger

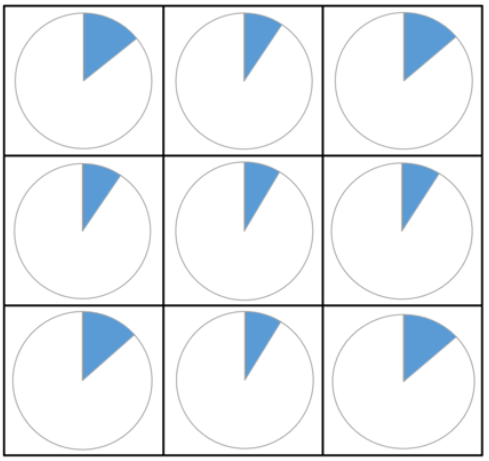

FIGURE 7.6: Liquid flow distribution in 9 planes at the top of the catalyst bed to the simulation domain with 40cm of depth.

depth. Also it is important to note that right above the top of the catalyst bed, the velocities are lower in the case with larger depth than the opposite case. A better analysis of the phases behavior in the dispersion zone is left as future work.

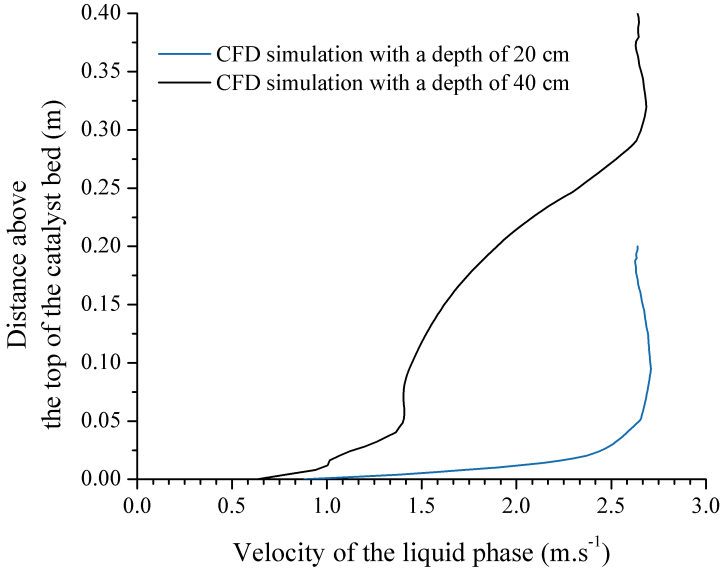

FIGURE 7.7: Velocity profile of the liquid phase above the top of the catalyst bed.

Chapter 8

Assessment of performance of a 1-D VGO-hydrocracking reactor using a non-homogeneous inlet profile

A one dimension mathematical model was developed for a VGO-hydrocracking reactor to evaluate the approximate performance of a catalyst bed when at the top of the reactor some of the non-homogenous hydrodynamic profiles obtained in the previous chapters are used. To describe the decomposition of the VGO by the hydrocracking reactions was chose to use a reaction mechanism based on five lumps (or pseudo-components)[34] proposed by Ancheyta for vacuum residue, the hydrocracking reactions of vacuum residue were obviate because there is an absence of vacuum residue in the feedstock. The reaction mechanism used is composed by four pseudo-components (VGO, Distillates, Naphtha and Gas) and six reactions. The final reaction pathways used in the one-dimension model of the VGO-hydrocracking reactor are showed at the Figure 8.1.

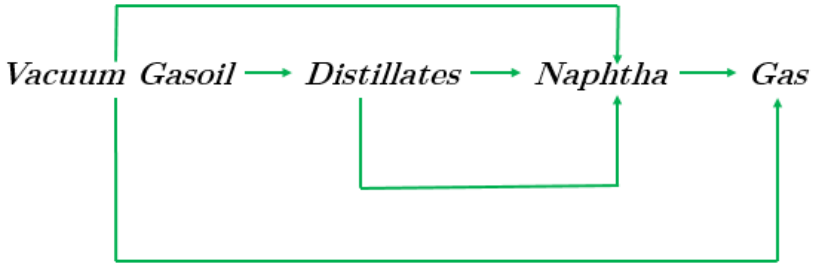

FIGURE 8.1: Reaction mechanism used on the 1-D simulation of VGO-hydrocracking reactor.

8.1 Model development

The mathematical model for the hydrocracking catalyst bed was built using an axial mass balance for each pseudo-component and hydrogen. The reaction mechanism do not consider the hydrogen as a component because was built with a common assumption for hydrocracking processes, under this assumption the reaction rates are independent of the hydrogen concentration since this concentration is in excess. However the model built for the hydrocracking catalyst bed can handle the consumption of hydrogen, using the C/H ratios of each pseudo-component the stoichiometric coefficients of the reactions were calculated, the coefficients allowed to introduce to the model the hydrogen cosumption rate.

The final mathematical model of the hydrocracking catalyst bed is composed by six differential equations, five differential equations for the mass balances of each pseudo-component and the hydrogen, and another equation for the energy balance. The set of differential equations is presented below.

$$\frac{dF_i}{dV} = R_i$$

$$R_i = \sum_{j=1}^{6} \zeta_{ij}\gamma_j$$

$$\frac{dT}{dV} = \frac{\sum_{j=1}^{6} \Delta H_{rxn_j}\gamma_j}{\sum_{i=1}^{5} F_i C_{p_i}}$$

To resolve the differential equation system was used the ordinary differential equation solver MATLAB routine *ode15s*, this routine can be used on stiff problems if needed. One boundary condition needs to be specified in the mathematical model (since is a 1-D model), the boundary condition was placed at the the inlet of the reactor, at the inlet is necessary to specify the flow of each component in the model (there are 5 components including the hydrogen) and the temperature. In the CFD simulations was assumed that the only components flowing were the VGO and the hydrogen, thereby the mass flow of the other components were assumed like 0 at the inlet of the catalyst bed.

8.1.1 Assumptions

The assumptions made to develop the hydrocracking reactor mathematical model are:

1. The rate of reactions are independent of the hydrogen concentration since the concentration is in excess. This means that all the reactions that are involved on the hydrocracking reaction mechanism are first order reactions.

2. The heat losses are negligible and the VGO-hydrocracking reactor operates at adiabatic condition.

3. Diffusional resistances are absent.

4. Steady state operation.

5. The reactor works on a plug flow pattern.

8.1.2 Fluid properties

A pseudo-component (or lump) is defined as fictional group of molecules with similar molecular weight and chemical characteristics, this concept allows to reduce the complexity of some systems in chemical reaction engineering where are involved thousand of different molecules (like the VGO-hydrocracking reactor) grouping them in pseudo-components. TTo characterize the pseudo-components used of the VGO-hydrocracking reactor simulation were needed the API gravity and a distillation curve, these data allowed to obtain the set of properties for each pseudo-component.

In the absence of experimental data to characterize the pseudo-components of the reaction pathway, literature data was used instead [3, 35–38]. A first search of information in the literature allowed to identify ranges of API gravity and temperature for each pseudo-component. The results of the literature search can be seen at the Figure 8.2, 8.3 and 8.4.

From all the distillation curves found in literature two curves were selected to characterize the Distillates and Naphtha pseudo-components, the selected ones were those curves with the wider range of temperature, hoping that a wider range allows a better characterization of the of the pseudo-components. On the other hand, the Gas pseudo-component it is commonly characterized using a percentage distribution of the species that composes the gas mixture, in a VGO-hydrocracking process the gas mixture has a high concentration of methane (70% on a mass basis) [4], the pseudo-component Gas was assumed as methane because has a higher concentration than the rest of components in the gas mixture. At the Figure 8.5 are presented the distillation curves used on Aspen HYSYS to calculate the properties of the pseudo-components.

Properties like density, viscosity, surface tension and other important properties that are needed in the simulations processes were calculated in Aspen HYSYS indirectly

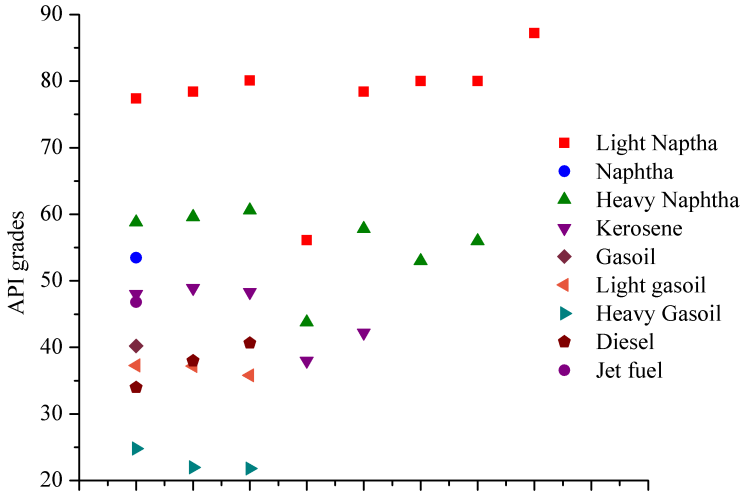

FIGURE 8.2: Dispersion plot of the API grades found in literature for different peuso-components of the hydrocracking process.

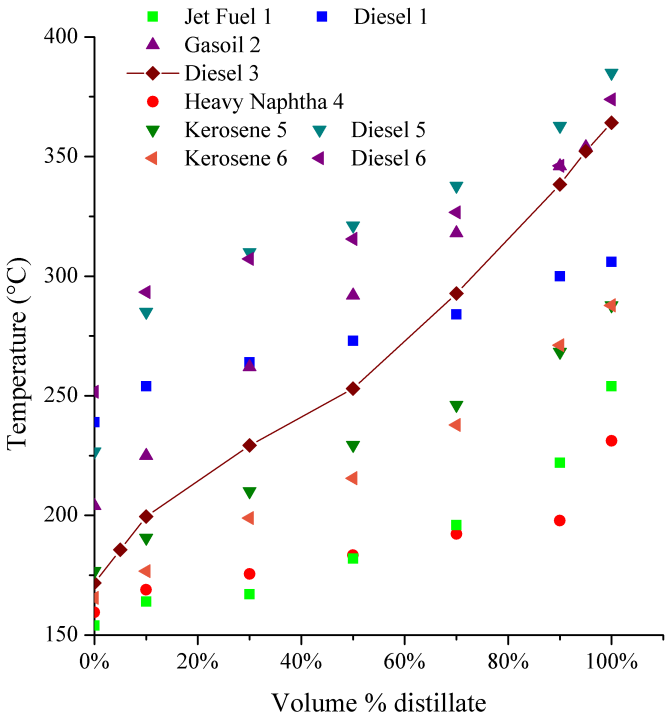

FIGURE 8.3: Dispersion plot of the ASTM D86 found in literature for different peuso-components similar to Distillates of the hydrocracking process. Data number: 1-[35], 2-[36], 3-[37], 4-[3], 5-[38], 6-[38].

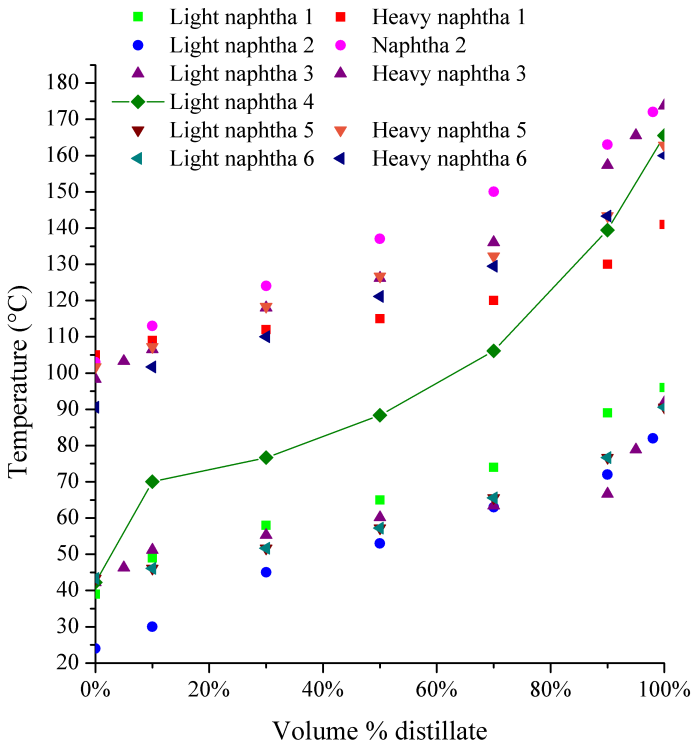

FIGURE 8.4: Dispersion plot of the ASTM D86 found in literature for different peuso-components similar to Naphtha of the hydrocracking process. Data number: 1-[35], 2-[36], 3-[37], 4-[3], 5-[38], 6-[38].

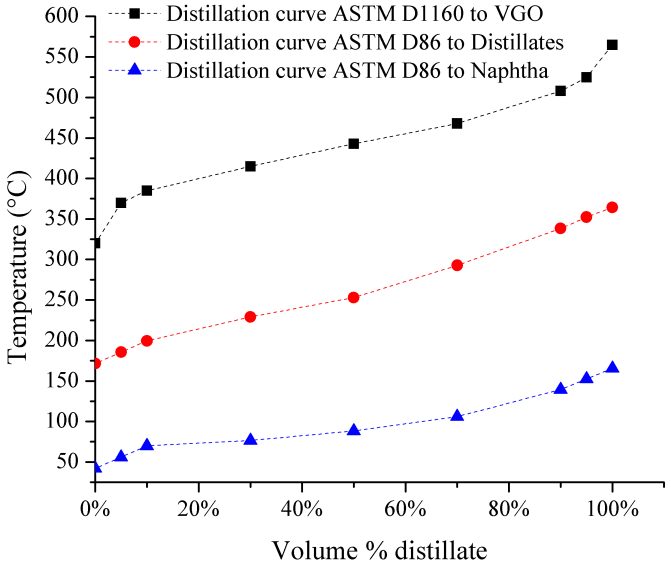

FIGURE 8.5: TBP curves used to obtain the properties of the lumps in the hydrocracking reaction mechanism. Distillate and naphtha are ASTM D86 curves and Feed curve is an ASTM D1160

using the API gravity and the distillation curve of each pseudo-component. To calculate the properties used in the simulations there is intermediate step, in this step empirical correlations are used to estimate thermodynamic properties that allow to calculate all other properties, in Table 8.1 can be seen the thermodynamic properties as well as the correlation used to estimate them.

TABLE 8.1: Correlations used by Aspen HYSYS to characterize a pseudo-component.

Property	**Correlation**
Molecular weight	Extended Twu critical
Specific gravity	Constant Watson K
Critical temperature	Twu critical property correlation
Critical pressure	Twu critical property correlation
Acentric factor	Twu critical property correlation
Ideal enthalpy	Lee Kesler

The kinetics constants of the reaction mechanism were obtained by numerical optimization, this kinetics constants have the particularity that were obtained using a data base of hydrocracking yields that was built with literature data and operate over a wider range of operation conditions, the procedure used to obtain the constants on the Table 8.2 is detailed in [39].

TABLE 8.2: Kinetic constants of the four lumps mechanism reaction to hydrocracking of VGO

Reaction	$log_e(k)$ (h^{-1})	E_a $(kJ.mol^{-1})$
1	10.1277	59.7720
2	27.9983	213.9262
3	19.2296	216.9726
4	5.5026	33.0237
5	3.7916	31.7994
6	24.0114	281.8131

8.2 Validation process

Previously to use the 1-D VGO-hydrocracking model over the CFD simulation results it was necessary to validate if the model built represents correctly a hydrocracking process. To validate the mathematical model was used at same conditions as the industrial size hydrocracking reactor simulated by Mohanty in 1990 [32]. Mohanty in his research work simulated a two-stages hydrocracking process, which is a special configuration commonly used to improve the conversion of the feedstock in refinery by using a second hydrocracking reactor in series with hydrotreating-hydrocracking reactor and a distillation tower. In this kind of configuration the first reactor is used mainly to eliminate the heteroatoms in the feedstock but but some hydrocracking reactions also take place, the unconverted

feedstock is separated at the distillation tower and goes to the second hydrocracking reactor, in the second reactor there are catalyst beds with high conversion catalyst, in different conditions, use this kind of catalyst it would be economically non-viable because has a high cost and can easily be fouled in presence of high heteroatoms concentrations.

The second Mohanty hydrocracking reactor comprises three catalytic beds and two hydrogen quenches between beds. The length of each bed in the reactor is not specified, instead it was assumed that the three beds have the same length. For each catalyst beds were solved the mass balances of each component and the energy balance, for the quenches were solved the mas balance of the hydrogen component (the other pseudo-components remain constant) and the energy balance to find the inlet temperature to the next bed.

Figure 8.6 and 8.7 are parity plots where the experimental data taken from the Mohanty were compared against the calculated results by the 1-D hydrocracking reactor model, the Figure 8.6 shows that the model built was capable of represent the consumption most important pseudo-components (feedstock and distillates) with an error below 10% but have low accuracy trying to represent the yields of the light pseudo-components (gas and naphtha). It is important to note that the reaction mechanism used on the simulation was optimized to represent a wide range of operation conditions in hydrocracking process, then it is expected that the model has some issues to represent accurately small values like the yields of the light pseudo-components. Even though the limitation of the mathematical model to represent the yields of the lighter component it is possible to state that the 1-D mathematical hydrocracking model it is approximately correct in describing the behavior and estimating the yields of the pseudo-components used in the reaction mechanism.

Finally it was necessary to examine the results obtained in the energy balance, at first sight Figure 8.7 shows good agreement among the experimental and calculated data (the error is below 2.5%), but in terms of temperature, differences among data above 1% could be considered as unacceptable to be considered a reliable simulation, however it is necessary to remark that the model will be used to give a general perspective of the approximate behavior of the species in a hydrocracking process when there is a change in the hydrodynamic conditions at the inlet of the reactor, under this perspective the simulation results in mass and energy balances seem to suitable to fulfill the aim proposed.

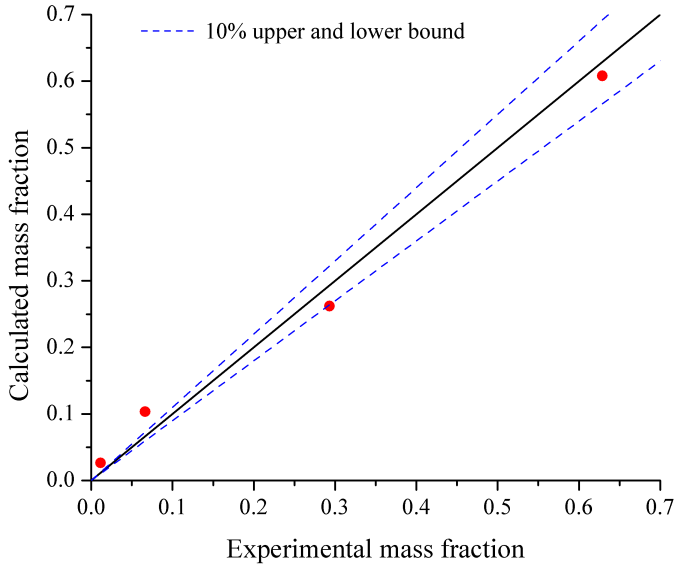

FIGURE 8.6: Parity plot of the mass balance, comparison between the calculated data against the experimental data measured by Mohanty.

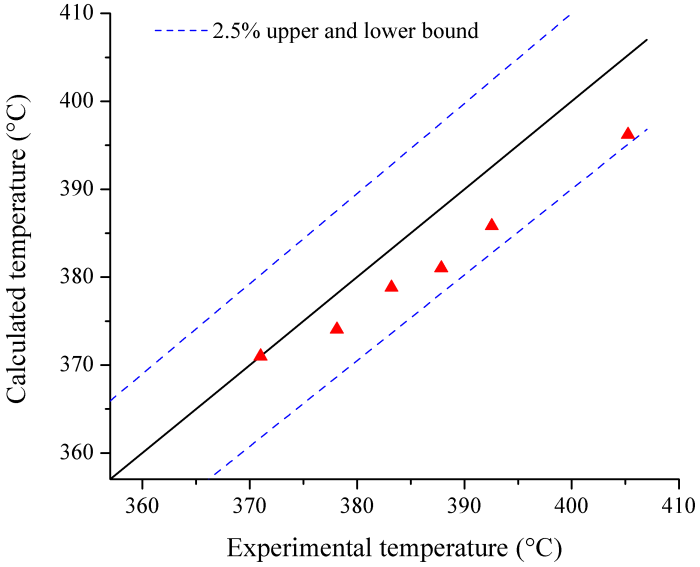

FIGURE 8.7: Parity plot of the energy balance, comparison between the calculated data against the experimental data measured by Mohanty.

8.3 CFD modeling

The liquid distribution at the top of the catalyst bed to be evaluated with the 1-D hydrocracking model was obtained by a CFD simulation similar to the one built in chapter 6, however the improvements obtained at the chapter 7 were implemented. As can be seen in chapter 7, the CFD simulations showed that a VLD unit with a ratio of 0.83 minimizes the liquid phase flow in contact with the wall and there is an improvement of the liquid distribution in the dispersion zone when there is a distance of $40cm$ between the distribution tray and the top of the catalyst bed, both conclusions of the chapter 7 can be expressed as changes at the inlet boundary conditions and at the geometry over the new CFD simulation.

The liquid phase volume fraction and the velocity profile at the inlet boundary conditions were taken from the CFD simulation of the VLD unit with a ratio of 0.83 between the separation plate height and the total VLD height, both profiles can be seen in the Figures 8.8 and 8.9, respectively.

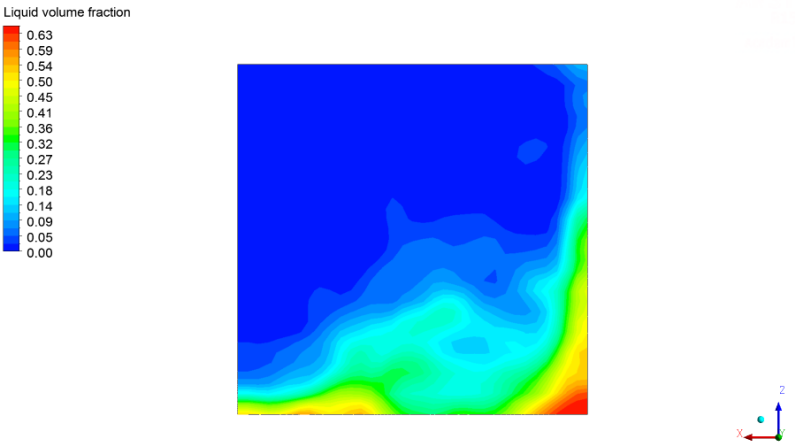

FIGURE 8.8: Liquid volume fraction profile obtained after an averaging process to different times.

The same simulation domain in chapter 6 was used again, as it was mentioned previously the depth was increased to enhance liquid distribution, thus the dimension of the new simulation domain are 0.674x0.674x0.4m. The CFD simulation in this chapter remains quite similar to the one presented at the chapter 6, models, properties, time step and bed properties keep the same values; if more information is needed in the section CFD modeling in chapter 6 the CFD simulation is extensively explained, in this section are only explained the changes made over the original simulation.

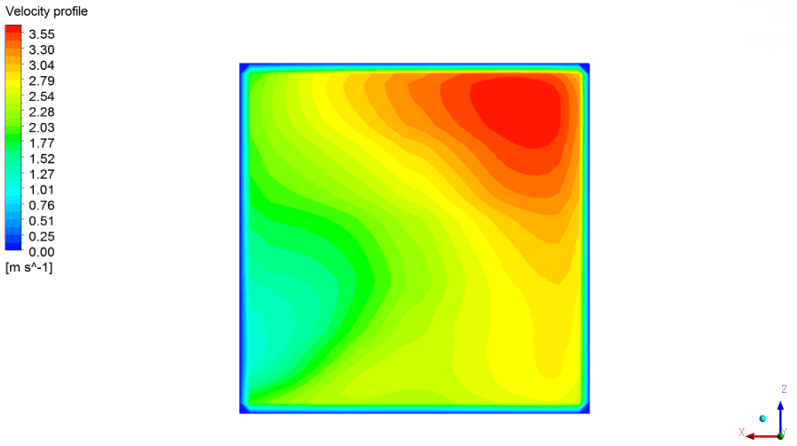

FIGURE 8.9: Velocity profile obtained after an averaging process to different times.

8.4 Results

As previously noted the 1-D hydrocracking model was used to bring an approximation of the behavior of the reactor catalyst bed when there is a non-homogeneous distribution of the liquid phase at the inlet, a liquid distribution profile is composed by the velocity profile of the phases and the volume fraction profile of the liquid phase. From the CFD simulations two liquid distribution profiles were obtained, besides three more inlet profiles with homogeneous distribution of the liquid phase were evaluated using the 1-D hydrocracking reactor model. The cases evaluated are:

- VLD units oriented in the same direction.
- VLD units oriented in different directions.
- Homogeneous distribution with a $Q_{in} = 0.02523 m^3.s^{-1}$.
- Homogeneous distribution with a $Q_{in} = 0.02540 m^3.s^{-1}$.
- Homogeneous distribution with a $Q_{in} = 0.02460 m^3.s^{-1}$.

As noted at chapter 6 the models used for each phase at the dispersion zone simulation are in transient form, then to obtain a characteristic liquid distribution at the top of the catalyst bed an averaging process through time was needed. The liquid distribution profiles were obtained from a surface at $5cm$ below the top of the catalyst every 150 time steps ($0.150s$) during 3000 time steps ($3s$) after the PSS was reached in the CFD simulation. The liquid distribution profiles at different times were saved in an ASCII format and then were read using MATLAB, then the variables of the profile (velocities

and liquid phase volume fraction) were averaged through time to obtain the characteristic profile of the CFD simulation.

The surface selected to obtain the liquid distribution profiles is composed by more than 10000 cells, which implies a substantial amount of data to be processed, in order to reduce the computational cost, a sample of the total data composed by a certain number of cells (not less than 800) were randomly taken, the number of cells in the sample increased until the mean and the standard deviation of the sample data are approximately the same as the total data of the surface. The 1-D hydrocracking model was applied over the sample of randomly taken cells. A similar process is applied on the homogenous distributions to avoid use the 1-D hydrocracking model on too many cells.

In Figure 8.10 are plotted the conversion obtained from the 1-D hydrocracking model for each of cells in the sample against the residence time, three important conclusions can be obtain from the Figure 8.10:

- as expected all the homogenous distribution are a point in the graph, on the other hand the profiles obtained from the CFD simulations have a wide range of residence times, this means that the residence time to the homogeneous profile is practically the same for all the cells.
- there is not a large difference between the configuration where VLD units are oriented in the different directions with the configuration where the VLD units are oriented in the same direction.
- as expected there is a linear correlation between the residence time and the conversion.

In Table 8.3 are the global values for conversion, yield of distillates, yield of naphtha and yield of gas, when those values were analyzed was found that a better conversion did not mean better yield of distillates, which means more consumption of feedstock leads to less production of distillates, because there is no temperature control inside the reactor the higher conversions will always be related with higher temperatures, the increasing temperature leads to increase both the rate of production and consumption of distillates and also to increase the rate of production of the other products. The behavior previously explained can be seen at the Figures 8.11,8.12 and 8.13, in those Figures also can be seen that to the operation range of temperature in the studied system there is an almost linear correlation between the yield of the distillates and the temperature, but linear correlation more evident when the yield of the distillates is plotted against the conversion.

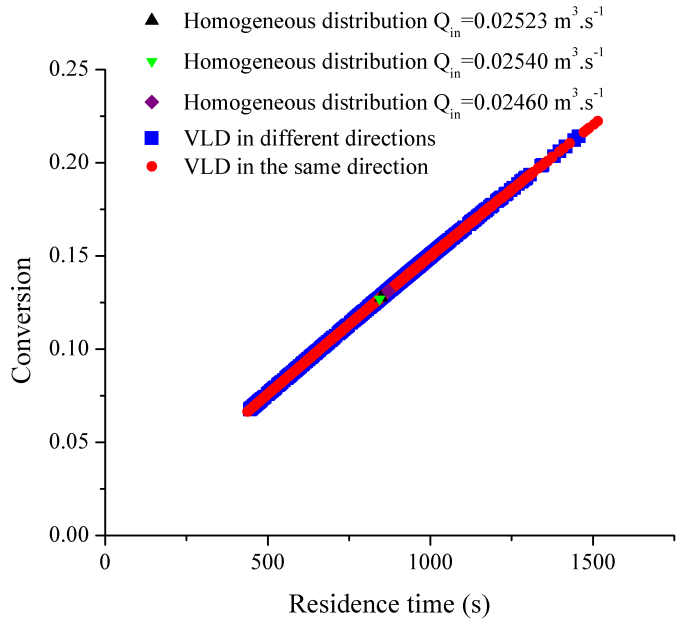

FIGURE 8.10: Conversion in function of the residence time to cells randomly selected in the cases evaluated.

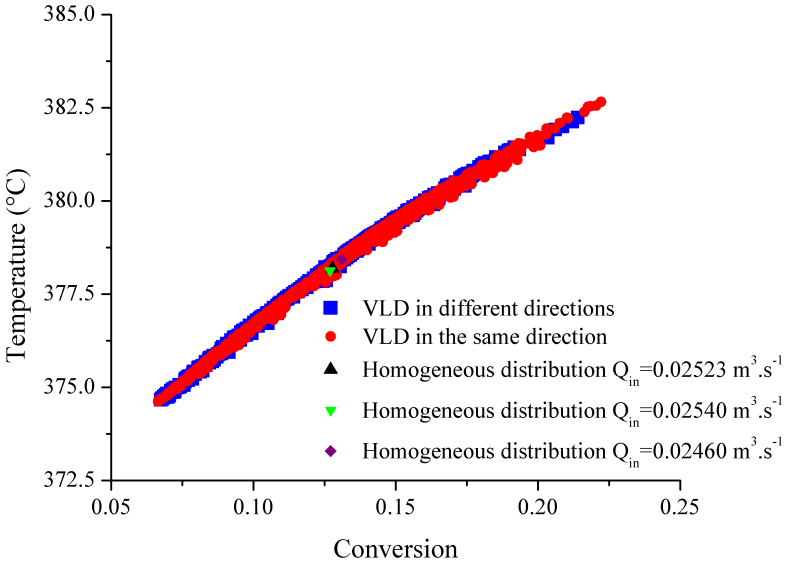

FIGURE 8.11: Conversion in function of the temperature to cells randomly selected in the cases evaluated.

TABLE 8.3: Global values of conversion, and products yields to the evaluated cases.

	Mass flux of feed at inlet ($kg.m^{-2}.s^{-1}$)	Conversion	Yield of distillates	Yield of naphtha	Yield of gas
VLD units oriented in the same direction	3.1737	0.1284	0.9104	0.1006	0.0258
VLD units oriented in different direction	3.1738	0.1284	0.9106	0.1004	0.0257
Homogeneous distribution with $Q_{in} = 0.02523$	3.1857	0.1278	0.9169	0.0951	0.0244
Homogeneous distribution with $Q_{in} = 0.02540$	3.1154	0.1311	0.9141	0.0975	0.025
Homogeneous distribution with $Q_{in} = 0.02460$	3,2172	0.1269	0.9176	0.0945	0.0242

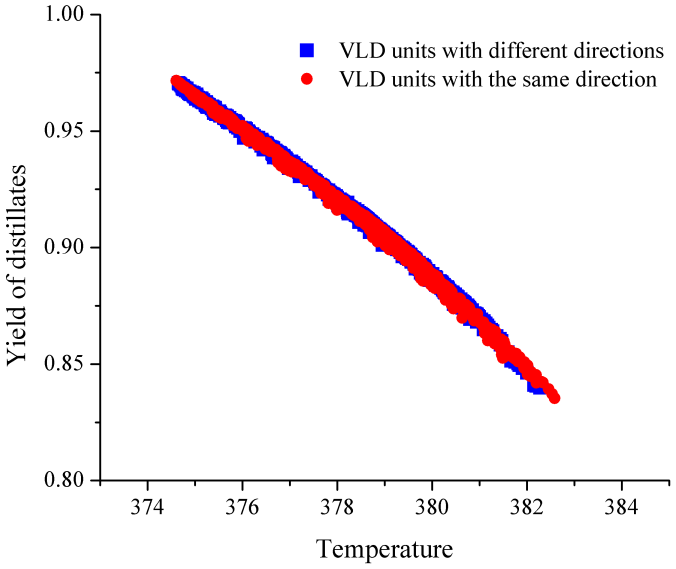

FIGURE 8.12: Yield of the distillates in function of the temperature to cells randomly selected in the cases evaluated.

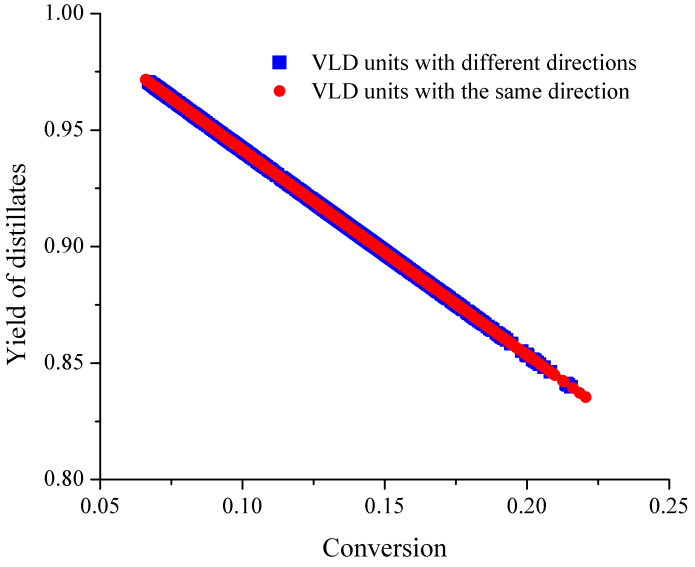

FIGURE 8.13: Yield of the distillates in function of conversion of the feedstock to cells randomly selected in the cases evaluated.

As can be seen at the Figures 8.11 and 8.14, in the same way as the conversion there is no significant difference among the temperatures obtained for the cases with homogenous distribution with the 1-D hydrocracking reactor model. To the cases with non-homogeneous profiles a temperature distribution is obtained with temperature values 3 or 5 ^oC above or below of the temperatures obtained for the homogenous distribution. The 1-D hydrocracking model cannot predict the real temperature at the outlet because the heat transfer between cells is not covered in the model, the temperature distribution as in Figure 8.15 is a tool formulated in the model to identify potential zones with high temperature, to observe if there are difference between non-homogeneous profiles or to propose ranges of probable temperatures at the outlet of the VGO-hydrocracking reactor.

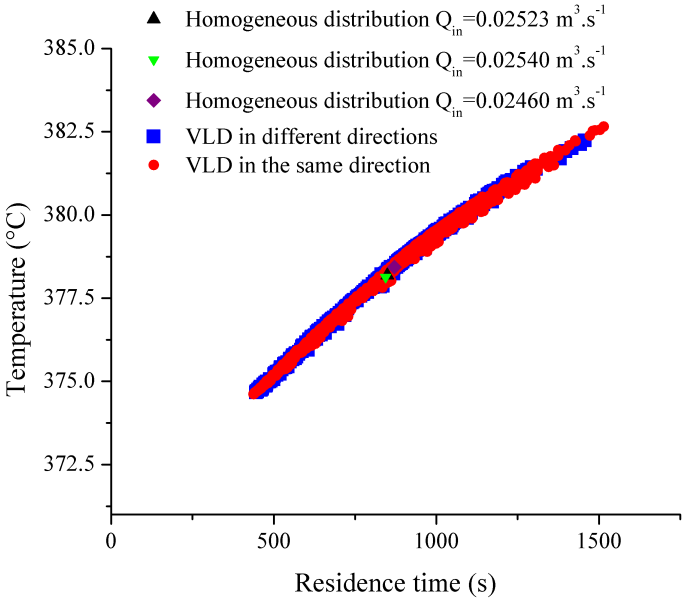

FIGURE 8.14: Temperature at the outlet of the 1-D VGO-hydrocracking reactor model as function of the residence time.

Finally the liquid distributions obtained from the CFD simulations were compared against a profile with a high maldistribution (bypassing), in this profile the liquid moves at higher velocities at the center of the surface. In the Figure 8.16 the mass flux of the feed is plotted against the conversion, it is clear that the maldistribution profile has the widest range of mass flux; in some points it is even reached a conversion of 1 but in those cells the mass flow near to 0. This means that wider the range of mass flux worse the liquid distribution at the top of the catalyst bed. The conclusion remains when the Figure 8.17 was analyzed, in this figure is plotted the residence time against conversion, also it is important to note that the linear dependence of the conversion with the residence time is lost when the fluids have a residence higher than 4000s. Both figures show an important fact, even if the profiles generated by the VLD units are quite different

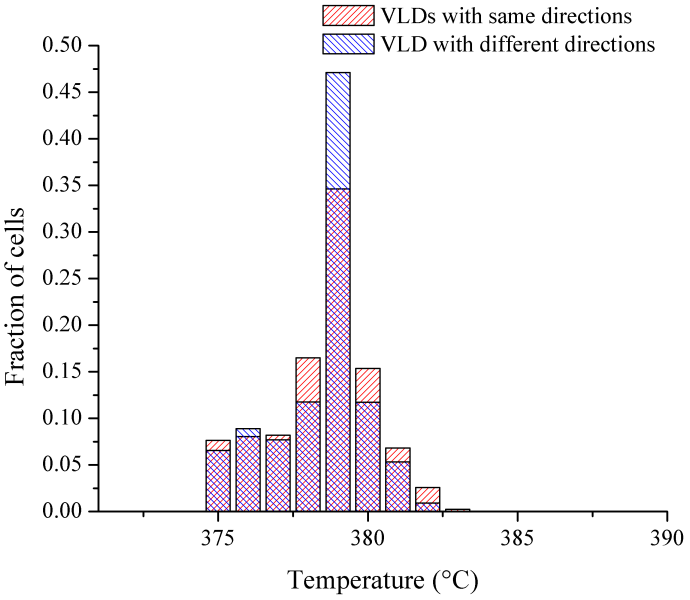

FIGURE 8.15: Distribution plot of temperatures at the outlet of the 1-D VGO-hydrocracking model.

from the ideal-homogeneous distribution, when compared against a profile with a high maldistribution it can be concluded easily that the VLD units provide liquid distribution profiles near to the desired standards.

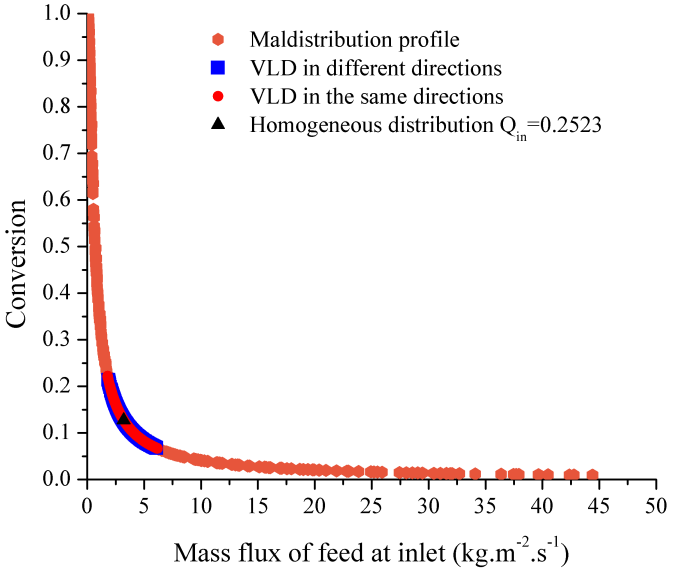

FIGURE 8.16: Evaluated cases compared against a profile with a high maldistribution in a plot of conversion as function of the mass flux of the feedstock at the inlet.

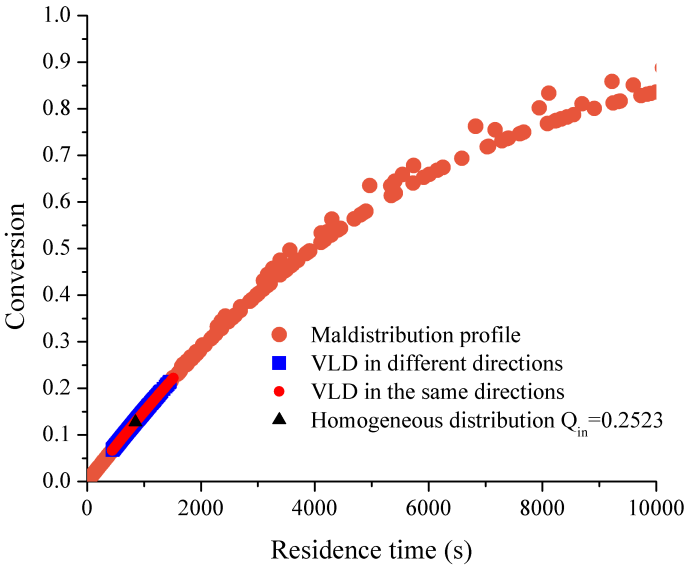

FIGURE 8.17: Evaluated cases compared against a profile with a high maldistribution in a plot of conversion as function of the residence time.

Chapter 9

Conclusions

The liquid flow maldistribution was successfully identified as a bottleneck to the VGO-hydrocracking reactor operation using literature data, this operational limitation was minimized through CFD simulation on three points of the distribution system, in those points the behavior of the phases was accurately captured as it was showed by the validation processes done on the proposed simulations.

A successfully CFD simulation of a VLD unit was proposed, previously to this work there was not a CFD simulation for this kind of device in the open literature, the simulation proved be able to represent experimental data found in the literature as well as similar behaviors observed on the experimental setups.

To enhance the liquid distribution at the top of the catalyst bed parameter variation processes were done over the VLD unit and the dispersion zone, at the VLD unit the best liquid distribution was obtained with an inner separation plate with a height of $25cm$, however by modifying the height of the inner wall only could minimize the liquid flow in contact with the wall, new modifications for the VLD unit are needed to eliminate that phenomenon. At the dispersion zone the liquid distribution was enhanced by increasing the distance between the distribution tray and the top of the catalyst bed from 20 to $40cm$, it is necessary to identify if increasing the distance between the distribution tray and the top of the catalyst bed always enhance the liquid distribution or otherwise there is a limit for the dispersion of the liquid phase.

A 1-D VGO-hydrocracking model was built in MATLAB, the properties of the pseudo-components used in the model were calculated using ASPEN Hysys and literature data (distillation curves and API gravity). A validation process showed that the model is able to represent adequately the behavior of a hydrocracking process. The VGO-hydrocracking model was used to evaluate the liquid distribution obtained from a CFD

simulation with all the improvements found by the parameter variation processes done. This evaluation showed that the liquid distribution generated by a VLD unit operates near to the homogeneous liquid distribution condition, using this kind of devices to mix the phases a slightly better global conversion is achieved but in expense of reach worse yields to the distillate product than homogenous liquid distribution condition.

The final configuration that ensures the best liquid distribution at the top of the catalyst bed to the conditions studied in this work is: a VLD unit with a height of $30cm$ and intern separation plate of $25cm$. The optimal separation between the distribution tray and the top of the catalyst zone is $40cm$, at the distribution tray the VLD units can be aligned all of them in the same direction to ease the building process because the alignment did no have an important role over the liquid distribution.

Bibliography

[1] Escenarios de Oferta y Demanda de Hidrocarburos en Colombia. Technical report, Unidad de Planeación Minero Energética, 2012.

[2] Edward Furimsky. Selection of catalysts and reactors for hydroprocessing. *Applied Catalysis A: General*, 171(2):177–206, jul 1998.

[3] David S. J. Stan Jones and Peter R. Pujadó, editors. *Handbook of Petroleum Processing*. Springer Netherlands, Dordrecht, 2006.

[4] Jorge Ancheyta, Sergio Sánchez, and Miguel A. Rodríguez. Kinetic modeling of hydrocracking of heavy oil fractions: A review. *Catalysis Today*, 109(1-4):76–92, nov 2005.

[5] Muthanna H. Al-Dahhan, Faical Larachi, Milorad P. Dudukovic, and Andre Laurent. High-Pressure Trickle-Bed Reactors: A Review. *Industrial & Engineering Chemistry Research*, 36(8):3292–3314, aug 1997.

[6] Milorad P. Dudukovic. *Ullmann's Encyclopedia of Industrial Chemistry*. Wiley-VCH Verlag GmbH & Co. KGaA, Weinheim, Germany, jun 2000.

[7] C. Marcandelli, A. S. Lamine, J. R. Bernard, and G. Wild. Liquid Distribution in Trickle-Bed Reactor. *Oil & Gas Science and Technology*, 55(4):407–415, jul 2000.

[8] Charles N. Satterfield. Trickle-bed reactors. *AIChE Journal*, 21(2):209–228, mar 1975.

[9] Y. Jiang, M.R. Khadilkar, M.H. Al-Dahhan, and M.P. Dudukovic. Two-phase flow distribution in 2D trickle-bed reactors. *Chemical Engineering Science*, 54(13-14):2409–2419, jul 1999.

[10] Prashant R. Gunjal, Vivek V. Ranade, and Raghunath V. Chaudhari. Liquid Distribution and RTD in Trickle Bed Reactors: Experiments and CFD Simulations. *The Canadian Journal of Chemical Engineering*, 81(3-4):821–830, may 2003.

[11] C. Boyer, A. Koudil, P. Chen, and M.P. Dudukovic. Study of liquid spreading from a point source in a trickle bed via gamma-ray tomography and CFD simulation. *Chemical Engineering Science*, 60(22):6279–6288, nov 2005.

[12] Prashant R. Gunjal, Madhavanand N. Kashid, Vivek V. Ranade, and Raghunath V. Chaudhari. Hydrodynamics of Trickle-Bed Reactors: Experiments and CFD Modeling. *Industrial & Engineering Chemistry Research*, 44(16):6278–6294, aug 2005.

[13] Yi Jiang, Jing Guo, and Muthanna H. Al-Dahhan. Multiphase Flow Packed-Bed Reactor Modeling: Combining CFD and Cell Network Model. *Industrial & Engineering Chemistry Research*, 44(14):4940–4948, jul 2005.

[14] A. Attou, C. Boyer, and G. Ferschneider. Modelling of the hydrodynamics of the cocurrent gasliquid trickle flow through a trickle-bed reactor. *Chemical Engineering Science*, 54(6):785–802, mar 1999.

[15] Prashant R. Gunjal and Vivek V. Ranade. Modeling of laboratory and commercial scale hydro-processing reactors using CFD. *Chemical Engineering Science*, 62(18-20):5512–5526, sep 2007.

[16] Amir Heidari and Seyed Hassan Hashemabadi. CFD simulation of isothermal diesel oil hydrodesulfurization and hydrodearomatization in trickle bed reactor. *Journal of the Taiwan Institute of Chemical Engineers*, apr 2014.

[17] Amir Heidari and Seyed Hassan Hashemabadi. CFD study of diesel oil hydrotreating process in the non-isothermal trickle bed reactor. *Chemical Engineering Research and Design*, sep 2014.

[18] Lars Bargsteen Møller, Christian Halken, Jens A. Hansen, and Jesper Bartholdy. Liquid and Gas Distribution in Trickle-Bed Reactors. *Industrial & Engineering Chemistry Research*, 35(3):926–930, jan 1996.

[19] Arunabha Kundu, Anil K Saroha, and K.D.P Nigam. Liquid distribution studies in trickle-bed reactors. *Chemical Engineering Science*, 56(21-22):5963–5967, nov 2001.

[20] N.A Tsochatzidis, A.J Karabelas, D Giakoumakis, and G.A Huff. An investigation of liquid maldistribution in trickle beds. *Chemical Engineering Science*, 57(17):3543–3555, sep 2002.

[21] Arnab Atta, Shantanu Roy, and Krishna D.P. Nigam. Investigation of liquid maldistribution in trickle-bed reactors using porous media concept in CFD. *Chemical Engineering Science*, 62(24):7033–7044, dec 2007.

[22] M. Bazmi, S.H. Hashemabadi, and M. Bayat. CFD simulation and experimental study of liquid flow mal-distribution through the randomly trickle bed reactors. *International Communications in Heat and Mass Transfer*, 39(5):736–743, may 2012.

[23] Z. Solomenko, Y. Haroun, M. Fourati, F. Larachi, C. Boyer, and F. Augier. Liquid spreading in trickle-bed reactors: Experiments and numerical simulations using EulerianEulerian two-fluid approach. *Chemical Engineering Science*, 126:698–710, apr 2015.

[24] Zeljko V. Kuzeljevic and Milorad P. Dudukovic. Computational Modeling of Trickle Bed Reactors. *Industrial & Engineering Chemistry Research*, 51(4):1663–1671, feb 2012.

[25] R. N. Maiti and K. D. P. Nigam. GasLiquid Distributors for Trickle-Bed Reactors: A Review. *Industrial & Engineering Chemistry Research*, 46(19):6164–6182, sep 2007.

[26] L. Raynal, F. Augier, F. Bazer-Bachi, Y. Haroun, and C. Pereira da Fonte. CFD Applied to Process Development in the Oil and Gas Industry A Review. *Oil & Gas Science and Technology Revue d'IFP Energies nouvelles*, aug 2015.

[27] Damian Enrique Ramajo, Santiago Marquez Damian, Marcela Raviculé, Maria M. Monsalvo, Mario Storti, and Norberto Nigro. Flow Study and Wetting Efficiency of a Perforated-Plate Tray Distributor in a Trickle Bed Reactor. *International Journal of Chemical Reactor Engineering*, 8(1), jan 2010.

[28] M. Martínez, J. Pallares, J. López, A. López, F. Albertos, M.A. García, I. Cuesta, and F.X. Grau. Numerical simulation of the liquid distribution in a trickle-bed reactor. *Chemical Engineering Science*, 76:49–57, jul 2012.

[29] Wei Du, Wenming Liu, Jian Xu, and Weisheng Wei. A novel modification of vapour-lift liquid distributor. *The Canadian Journal of Chemical Engineering*, 92(1):109–115, jan 2014.

[30] Mikael Per Daniel Nolin. Experimental Investigation , Model Examination , and Solver Validation of the Vapor Lift Tube Distributor Tray. (2), 2014.

[31] Frédéric Bazer-Bachi, Yacine Haroun, Frédéric Augier, and Christophe Boyer. Experimental Evaluation of Distributor Technologies for Trickle-Bed Reactors. *Industrial & Engineering Chemistry Research*, 52(32):11189–11197, aug 2013.

[32] S Mohanty, D.N. Saraf, and D. Kunzru. Modeling of a hydrocracking reactor. *Fuel Processing Technology*, 29(1-2):1–17, nov 1991.

[33] Octave Levenspiel. Basics of Non-Ideal Flow. In *Chemical reaction engineering*, chapter 11, pages 257–258. John Wiley & Sons, New York, EE.UU, 3 edition, 1999.

[34] Jeremías Martínez and Jorge Ancheyta. Kinetic model for hydrocracking of heavy oil in a CSTR involving short term catalyst deactivation. *Fuel*, 100:193–199, oct 2012.

[35] Xu ZhengLi, Li YongLin, and Li ChengLie. the Respliting of Hydrocracking Products. *Petroleum Science and Technology*, 18(9-10):1161–1173, nov 2000.

[36] Emir Ceric. *Crude oil, processes and products.* IBS-Saravejo, Sarajevo, Boznia - Herzegovina, 2012.

[37] Ai-Fu Chang, Kiran Pashinkanti, and Y.A Liu. *Refinery Engineering: Integrated Process Modeling and Optimization.* Wiley-VCH Verlag & Co, Weinheim, Germany, 2012.

[38] Mohamed A. Fahim, Taher A. Alsahhaf, and Amal Elkilani. *Fundamentals of Petroleum Refining.* Elsevier, 2010.

[39] L. C. López, A. Molina, J. J. Arias, and M. Kraft. Data Standardization Using an Extensible Mark-up Language (XML) to Estimate Kinetic Parameters for Refinery Processes. Case Study: Hydrocracking. In *Topical Conference on Refinery Processing*, Austin, TX, 2015.